BIOCHEMISTRY
including biophysical chemistry & molecular biology

Current Topic

pubs.acs.org/biochemistry

Combined Quantum Mechanics/Molecular Mechanics (QM/MM) Methods in Computational Enzymology

Marc W. van der Kamp* and Adrian J. Mulholland*

Centre for Computational Chemistry, School of Chemistry, University of Bristol, Bristol BS8 1TS, U.K.

ABSTRACT: Computational enzymology is a rapidly maturing field that is increasingly integral to understanding mechanisms of enzyme-catalyzed reactions and their practical applications. Combined quantum mechanics/molecular mechanics (QM/MM) methods are important in this field. By treating the reacting species with a quantum mechanical method (i.e., a method that calculates the electronic structure of the active site) and including the enzyme environment with simpler molecular mechanical methods, enzyme reactions can be modeled. Here, we review QM/MM methods and their application to enzyme-catalyzed reactions to investigate fundamental and practical problems in enzymology. A range of QM/MM methods is available, from cheaper and more approximate methods, which can be used for molecular dynamics simulations, to highly accurate electronic structure methods. We discuss how modeling of reactions using such methods can provide detailed insight into enzyme mechanisms and illustrate this by reviewing some recent applications. We outline some practical considerations for such simulations. Further, we highlight applications that show how QM/MM methods can contribute to the practical development and application of enzymology, e.g., in the interpretation and prediction of the effects of mutagenesis and in drug and catalyst design.

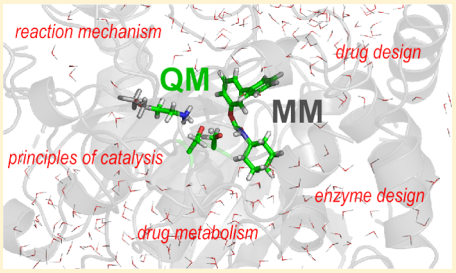

Enzymes are both essential and extraordinary due to their phenomenal capability to catalyze biochemical reactions efficiently, typically with high specificity and under mild, physiological conditions. Understanding how enzymes achieve these remarkable feats is not only one of the most important fundamental problems in biology, it will also contribute to a range of technological applications such as designing inhibitors that serve as lead compounds in drug discovery, predicting the metabolism of drugs, and designing catalysts for specific transformations. A wide variety of experiments in structural biology, enzyme kinetics, and mutagenesis have given insight into enzymes. Because of the complexity of enzymes and the difficulty of studying reactions in them, however, many questions and uncertainties remain, giving rise to many heated debates in enzymology. Computational modeling and simulation, with their unique potential to offer detailed, atomic-resolution insight into the dynamics and reactions of biomolecules,[1] can help resolve such controversial questions by interpreting, complementing, and expanding results obtained from experiment. Perhaps most obviously, calculations can study transition state structures, which are central to reactivity but cannot be studied directly by experiments on enzymes.

Computational enzymology can be defined broadly as the study of enzymes and their reaction mechanisms by molecular modeling and simulation. This field has matured rapidly in recent years, and increasingly experimental and computational enzymologists are collaborating to explain experimental data (see, e.g., refs 2 and 3) and use insights from modeling to guide further experiments. A number of different types of simulation have proved useful in computational enzymology. Combined quantum mechanics/molecular mechanics (QM/MM) methods have been involved in this field,[4,5] ever since the pioneering work of Warshel and Levitt in 1976.[6] The desire to model reactions within enzymes has been an important driving force in the development of QM/MM methods. This review will primarily focus on QM/MM methods in computational enzymology; other simulation and modeling methods are also important in this field. In particular, the empirical valence bond (EVB) approach (which typically uses a combination of molecular mechanics representations rather than a molecular mechanics and an electronic structure QM method) has provided many fundamental insights into enzyme catalysis.[7−9] Calculations that employ QM methods only[10] also provide a good route to modeling many enzyme mechanisms, differing from QM/MM calculations mostly in the size of the system that can be modeled. In this review, we discuss different types of QM/MM methods, their scope, and practical considerations in their application to modeling enzyme reactions. We indicate how QM/MM methods have contributed to debates on the sources of enzyme catalytic power and provide detailed insight into individual mechanisms. We further highlight how modeling of reactions with QM/MM methods is contributing to developments in drug design, drug metabolism, and biocatalyst design. QM/MM methods are also being applied to other types of problems in biomolecular science, e.g., in the calculation of spectroscopic properties, photochemistry, pK_a's, and predictions of ligand binding affinities in docking and free energy simulations,[11−17] but such applications are outside the scope of this review.

Received: February 19, 2013
Revised: April 2, 2013
Published: April 4, 2013

   dx.doi.org/10.1021/bi400215w | *Biochemistry* 2013, 52, 2708−2728

MODELING ENZYME-CATALYZED REACTION MECHANISMS WITH QM/MM METHODS

QM/MM methods are now widely applied to enzymes: since 2007, over 100 studies have been published every year (with 139 and 124 original articles published in 2011 and 2012, respectively[a]). It is therefore not possible to cover all or even a majority of recent QM/MM studies on enzymes in a short review. The level of detail, sophistication, and accuracy in these studies is generally increasing. This has been made possible by increased computer power, greater accessibility of software in which QM/MM methods are implemented, and developments in methodology. The principle of QM/MM approaches is to treat a small part of the system with a quantum mechanical (QM) method (i.e., a method that describes the electronic structure of molecules) and the rest of the system with a molecular mechanical method (i.e., a method that describes interactions between atoms using a simple potential energy function, a 'force field'[18]). The QM treatment allows modeling of the electronic rearrangements involved in the breaking and making of chemical bonds, while the MM treatment allows for the efficient inclusion of the wider environment and its effects on the reaction energetics. QM/MM methods as applied to enzymes have been described in detail elsewhere.[19,20] Two general types of QM/MM method are the *additive* approach ($E_{total} = E_{QM(QM)} + E_{MM(MM)} + E_{QM\text{-}MM\ interaction}$, with $E_{QM(QM)}$ the energy of the QM region according to the QM method, $E_{MM(MM)}$ the energy of the MM region according to the MM method, and $E_{QM\text{-}MM\ interaction}$ the interaction energy between the two regions) and the *subtractive* approach ($E_{total} = E_{MM,total} + E_{QM(QM)} - E_{MM(QM)}$, with $E_{MM,total}$ the energy of the total system and $E_{MM(QM)}$ the energy of the QM region as calculated by the MM method), as used in the ONIOM method.[21] In the subtractive approach, the active site region is modeled at the MM level, and choice of suitable MM parameters (e.g., atomic charges) for all states of the reaction is an important consideration, which may not be apparent to the unaware user. Until recently, calculations using the subtractive approach typically applied the more approximate 'mechanical embedding' scheme, whereas currently, most implementations of both approaches allow 'electrostatic embedding',[21] which takes into account the (often important) electrostatic influence of the MM region on the QM region, i.e., polarization of the QM region by the atomic charges of the MM region.

Five general aspects are important in planning a QM/MM calculation on an enzyme:[b]

(1) Choice of the QM method
(2) Choice of MM forcefield (including MM parameters required for the QM region)
(3) Partitioning of the system into QM and MM regions (including treatment of covalent bonds at the boundary)
(4) Type of simulation (e.g., a molecular dynamics simulation, or calculation of potential energy profiles), e.g., whether extensive conformational sampling will be performed
(5) Construction (and testing) of an accurate molecular model of the enzyme complex

The choice of QM method is crucial: the method should be suitable for the reaction of interest as well as computationally feasible for the type of simulation required. A plethora of different QM methods exists, ranging from fast, semiempirical methods (e.g., AM1, PM3, SCC-DFTB) to more accurate, but more computationally expensive, density functional (e.g., B3LYP) and molecular orbital *ab initio* (e.g., MP2, coupled-cluster) methods. Not all methods are applicable to all systems, either for reasons of accuracy, practicality (e.g., correlated *ab initio* methods are too expensive for routine application to transition metals, although this picture is changing[22]), or lack of parameters (e.g., for semiempirical methods). Generally (but not always), improved accuracy comes at the price of increased calculation expense. It is possible, however, to reparameterize approximate methods, or to apply simple corrections, to improve accuracy for specific reactions;[23−25] this can provide accurate methods for applications that require many energy evaluations, such as molecular dynamics simulations (*vide infra*). Also, newer semiempirical methods can offer increased accuracy and wider areas of application.[26−28] Correlated *ab initio* QM methods are useful in testing the accuracy of less computationally demanding QM methods (e.g., semiempirical, or density functional theory, DFT), because the latter can have important (and sometimes unsuspected) limitations for specific enzyme reactions.[29,30] For DFT calculations, inclusion of dispersion effects (e.g., by empirical corrections)[31] can be important for modeling reactions.[30,32]

The MM force field employed in a QM/MM study should be chosen such that it accurately describes the part of the system outside the QM region *and* its interactions with the QM region. For proteins, standard all-atom force fields such as CHARMM27, AMBER ff99 or ff99SB, and OPLS-AA are commonly used. Apart from selecting suitable QM and MM methods and a QM/MM approach, modeling an enzyme reaction with a QM/MM method requires several other important choices, such as deciding which atoms to include in the QM region, how to treat covalent bonds that cross the QM/MM boundary (e.g., introducing additional link atoms between MM and QM atoms, hybrid orbitals on MM atoms or a 'pseudobond' to replace the QM-MM covalent bond[33] — all these methods can give reasonable results), determining the protonation states of residues, and how (long-range) electrostatic interactions are treated. (The two latter choices apply to other types of biomolecular simulation also.) Again, it is advisable to test the influence of such choices on the results[29,34−37] in order to draw reliable conclusions. Recently developed methods allow relocating the QM-MM boundary on-the-fly (adaptive partitioning), which could help with some types of application.[38]

After preparing an atomic model of the enzyme and substrate (usually based on a X-ray crystal structure), the next step is to study the enzyme reaction in this model. An important outcome of such a study can be detailed structural information of the conformation that represents the highest energy during a reaction, the transition state (TS) structure. TSs are not directly accessible by experiment, due to their short lifetime and the complexity of enzymes, but are essential in understanding reactivity. Information on the enzyme−TS complex can also potentially be exploited in the design of enzyme inhibitors (e.g., drug leads)[39,40] and catalysts.[41−43] Various simulation techniques can be applied to model reaction pathways in enzymes and obtain TSs (see e.g., refs 19 and 20). Depending on the goals of the study, one can focus on obtaining (relative) potential energies, or alternatively free energies, for the reaction. A potential energy profile or minimum energy pathway (MEP) can be obtained by minimizing the energy of the system at several points along the reaction coordinate. The structure highest in energy on this MEP represents a TS structure. It must be noted that multiple enzyme−substrate

dx.doi.org/10.1021/bi400215w | *Biochemistry* 2013, 52, 2708−2728

conformations should ideally be considered when MEPs are calculated, because the barriers and TS structures for different starting conformations can differ significantly.[29,44,45] The barrier to reaction from a *free* energy profile can, in principle, be directly compared to an (apparent) activation free energy obtained from an experimental apparent first-order reaction rate constant (k_{cat}) using transition state theory (TST).[46] QM/MM modeling approaches, however, are not yet at the stage where quantitatively accurate free energy profiles, e.g., using high-level QM methods, can routinely be obtained. Free energy profiles ideally involve sampling of the structural fluctuations of the system. Sufficient sampling requires many calculations, which can be expensive for QM/MM methods. One strategy is to model the QM region using cheap, approximate methods (e.g., semiempirical QM). By comparing free energy and potential energy profiles obtained using such approximate methods, estimates of the activation entropy can be calculated. In turn, these can be added to the potential energy barrier from a high-level MEP, to estimate the activation free energy (see, e.g., refs 47−49). In favorable cases, QM/MM simulations can thereby calculate enzyme reaction barriers in quantitative agreement with experiment.[47] It is important to note, however, that qualitative agreement is often sufficient to distinguish between alternative mechanisms, determine substrate specificity, or assess the effect of mutations. A popular strategy that avoids using approximate QM methods to obtain QM/MM free energy differences involves taking points on the high-level MEP, fixing the QM region, and sampling the MM region around it extensively.[50] Fixing the QM region can be a serious limitation of this QM/MM-FE approach, but may be alleviated by reintroducing ways to sample conformations in the QM region.[51,52] Promising methodological developments use the QM/MM-FE principle to optimize the minimum *free* energy path of a reaction.[53] A different strategy is to perform Car−Parrinello molecular dynamics to sample conformations in the QM region.[54] This approach is typically limited to the use of generally less accurate gradient-corrected DFT methods (instead of hybrid DFT methods such as B3LYP), and even short simulations (∼10−100 ps) demand significant computational resources. More recently, Born−Oppenheimer QM/MM molecular dynamics simulations (e.g., using B3LYP) have also been employed to study enzyme mechanisms, typically by starting trajectories from different points of a previously calculated MEP.[55,56]

ESTABLISHING AND TESTING REACTION MECHANISMS

Typically, hypotheses for reaction mechanisms are developed based on structural, kinetic, and mutational data. Such experimental data, however, cannot give a complete picture of a reaction pathway and may be consistent with multiple possible mechanisms. Establishing the likely mechanism from experimental data alone can thus be far from trivial, as is clear from recent studies that indicate that several 'textbook' mechanisms may be wrong.[57,58] An example is hen egg white lysozyme (HEWL), the first enzyme to have its structure solved by X-ray crystallography.[59] Lysozyme is a glycosidase that catalyzes the hydrolysis of the glycosidic bond between *N*-acetyl-muramic acid (NAM) and *N*-acetyl-D-glucosamine (NAG) found in peptidoglycans that occur in the cell walls of (mainly Gram-positive) bacteria. The mechanism proposed by Phillips,[59] based on the structure of HEWL was commonly found in biochemistry textbooks and involves an oxacarbenium ion intermediate, formed by proton transfer from Glu35 to the glycosidic oxygen and the subsequent cleavage of the glycosidic bond. Later, crystallography and mass spectrometry experiments[57,60] indicated that instead, a previously proposed general mechanism by Koshland,[61] featuring a covalent intermediate with a bond between Asp52 and NAM, was preferred. These experiments required the use of HEWL mutants and/or unnatural substrates, leading to suggestions that it was unclear whether the covalent mechanism was used by wild-type HEWL. Bowman et al.[58] calculated QM/MM free energy profiles for the protonation of the glycosidic bond by Glu35 and subsequent cleavage, at the PM3-CHARMM27 level.[b] They observed spontaneous formation of the covalent intermediate with Asp52. The barrier for this reaction, using higher level QM corrections, appears reasonably consistent with experiment, and importantly the ionic intermediate was found to be significantly higher in energy than the covalent form. Together with the experimental findings, this provides convincing evidence that the Koshland-type mechanism is indeed correct. The TS for glycosidic bond breakage was found to be oxacarbenium ion-like; the very first QM/MM study of an enzyme concluded that lysozyme provides good electrostatic stabilization of such a species.[6] More recently, QM/MM studies have also revealed oxacarbenium ion-like TSs in 1,3−1,4-β-glucanase[62] and lipopolysaccharyl-α-1,4-galactosyltransferase C,[63] and covalent intermediate formation with a similar energy barrier was predicted for *Trypanosoma cruzi trans*-sialidase.[64]

Another example of an enzyme for which QM/MM modeling has helped elucidate the mechanism is citrate synthase. It catalyzes the first reaction in the citric acid cycle, the conversion of oxaloacetate into citrate, and is an important model for carbon−carbon bond formation in biology. The reaction features proton abstraction from acetyl-coenzyme A (acetyl-CoA), condensation of acetyl-CoA with oxaloacetate to form citryl-CoA, and hydrolysis of this stable intermediate to form citrate and CoA. The nature of the deprotonated acetyl-CoA intermediate was previously uncertain, with proposals of either an enolate or enol of acetyl-CoA or an 'enolic' form, with a so-called 'low-barrier' hydrogen bond between His274 and the acetyl oxygen. Early QM/MM modeling of the proton abstraction reaction, first at the AM1-CHARMM27[65] level and later the higher MP2/6-31+G(d)-CHARMM27[66] level, indicated that the enolate was energetically favored in the enzyme active site, with conventional (rather than 'low-barrier') hydrogen bonds from His274 and a conserved water molecule providing stabilization of this species (Figure 1).[66,67] Polarization of oxalacetate by the enzyme active site, observed spectroscopically,[68] was shown not to influence the activation barrier or stabilization of the intermediate significantly (by QM/MM calculations varying the polarization of oxaloacetate),[69] in contrast to some suggestions of its importance in catalysis. Recent high-level QM/MM calculations, at up to the local coupled-cluster level of QM theory, have provided further confirmation of the previous results.[29] Extensive testing of QM methods in that work further highlighted that the commonly used DFT-functional B3LYP does not correctly describe the energetics of the reaction due to overestimation of the enolate energy in the enzyme, whereas spin-component-scaled MP2[70] (SCS-MP2) is much more accurate. Subsequent QM/MM modeling using this method analyzed the enantioselective conversion of fluoroacetyl-CoA to fluorocitrate by CS, which causes the toxicity of the pesticide fluoroacetate.[49] Enantioselectivity arises from preferred abstraction of the pro-*R* proton

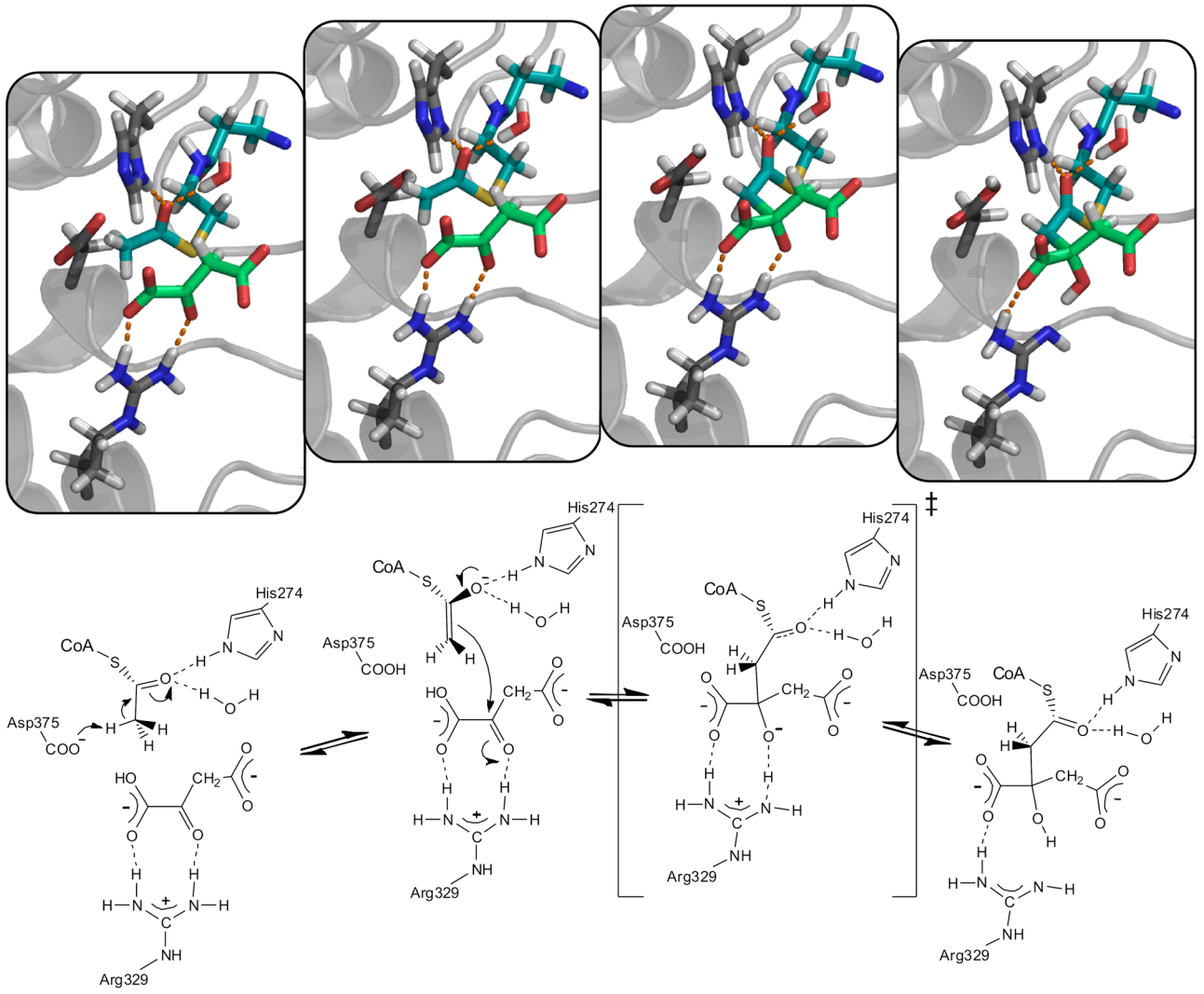

Figure 1. Reaction mechanism for carbon−carbon bond formation in citrate synthase as suggested by high-level QM/MM calculations. Proton transfer to Asp375 leads to an acetyl-CoA enolate intermediate (light blue), which subsequently attacks the carbonyl carbon of oxaloacetate (light green). To arrive at the citryl-CoA intermediate, an unusual proton transfer from Arg329 appears to be required. Structures are obtained by B3LYP/6-31+G(d)-CHARMM27 optimization.[76]

from the CFH_2 group. First, AM1-CHARMM27 MD simulations were performed with a model of the enzyme with oxaolacetate and fluoroacetyl-CoA bound (based on a crystal structure of chicken CS cocrystallized with acetyl-CoA and *R*-malate, PDB code 4CSC). This revealed that the fluoroacetyl-group can present both the pro-*S* and pro-*R* proton to the proton abstracting Asp375. Five TS structures for each reaction were then generated by AM1-CHARMM27 MD simulations along a reaction coordinate representing proton transfer ($r = d(O_{Asp375}H) - d(C_{FaCoA}H)$), which also gave estimates of the activation entropy (see above). These TS structures were subsequently used to obtain five potential energy profiles for each reaction along the reaction coordinate by optimizing the geometry at the B3LYP/6-31+G(d)-CHARMM27 level and calculating energies at the SCS-MP2/aug-cc-pVDZ-CHARMM27 level. The Boltzmann-weighted energy differences between the reactant state and enolate state for the pro-*R* and pro-*S* abstracting reactions indicated that pro-*R* abstraction, ultimately leading to the major product 2*R*,3*R*-fluorocitrate, was favored by ∼2 kcal mol^{-1}. This quantitatively agrees with the relative amounts of the major and minor products found in experiment and thereby indicates that the inherent energy difference between the two enolates that leads to the different fluorocitrate enantiomers is the main cause of the observed selectivity.

The high-level QM/MM modeling of the formation of the acetyl-CoA enolate in CS also indicated that this step may not be rate-limiting (i.e., that this step does not have the highest barrier along the whole reaction path).[29] This would mean that condensation of acetyl-CoA with oxaloacetate is probably rate-limiting for the mesophilic forms of the enzyme[71] (although condensation and hydrolysis will have similar barriers).[72] The mechanism for condensation is not clear, however, in particular regarding the necessary protonation of the former carbonyl oxygen of oxaloacetate. Suggestions include proton donation from one of the several histidines in the active site,[73,74] protonation coinciding with hydrolysis,[75] and, somewhat controversially, proton donation by Arg329,[74] which forms a hydrogen bond to the carbonyl oxygen. Van der Kamp et al. used QM/MM calculations to consider different proton donors in the reaction step.[76] Initial AM1-CHARMM27 level calculations indicated that Arg329 was best suited to donate

dx.doi.org/10.1021/bi400215w | *Biochemistry* 2013, 52, 2708−2728

the proton, which was subsequently confirmed by B3LYP/6-31+G(d)-CHARMM27 optimization of the whole condensation reaction path (including enolate formation, Figure 1), and ab initio QM/MM energy calculations: MP2/aug-cc-pVDZ-CHARMM27 energies are in agreement with experiment[77] (barriers of 14.2 kcal mol^{-1} and 14.7 kcal mol^{-1}, respectively), confirming the likelihood of proton donation by Arg329. This unusual role can help explain how citrate synthase avoids overstabilization of the citryl-CoA intermediate. Furthermore, the related loss of the salt-bridge between oxolacetate and Arg329 may trigger the opening of the active site required for the subsequent hydrolysis step, thereby indicating how chemical and conformational changes may be coupled.[76]

INVESTIGATING PRINCIPLES OF ENZYME CATALYSIS

The origin of the catalytic power of enzymes is still hotly debated. Many proposals have been put forward throughout the years, arguing for example the importance of 'low-barrier' hydrogen bonds,[78] so-called 'near-attack conformations',[79] enzyme dynamics,[80] and quantum tunneling[81] in some or all enzyme-catalyzed reactions. When considering such proposals (as pointed out, e.g., by Warshel et al.[82−84]) it is important to (a) define them rigorously in physical terms and (b) design and perform (*in silico*) experiments to test them. Molecular simulation is very useful for the latter, because it is possible to separate various effects in ways that are extremely difficult or impossible experimentally. For example, the contribution of quantum tunneling can be considered separately (*vide infra*).[85−88]

Almost all computational studies on enzyme reactions rely on transition state theory (TST) to connect to experimental rates of reaction. TST relates the rate constant of a reaction to the Gibbs free energy of activation ($\Delta G^{\ddagger}$). Modern TST includes a generalized transmission coefficient, which can incorporate the effects of recrossing of the energy barrier, quantum tunneling, and nonequilibrium contributions.[46] It is possible to include these effects in some simulations. The applicability of TST to enzyme-catalyzed reactions has been questioned (see, e.g., refs 89 and 90). The success of QM/MM, QM, and EVB modeling in calculating activation energies consistent with experiments for enzyme reactions, however (e.g., with high-level QM/MM calculations)[47,91] supports the applicability of TST.[92,93] So too, e.g., does the correlation observed between calculated barriers and experimental rate constants for some enzymes, such as phenol hydroxylase and *para*-hydroxybenzoate hydroxylase.[94−96] QM calculations on active site models give barriers that agree with experiment for many enzymes, in a TST framework.[10,97]

The potential role of protein dynamics is at the forefront of current debates on enzyme catalysis.[7,94,98−100] Although conformational changes related to protein dynamics are often crucial for enzyme turnover (e.g., allowing substrate binding and product release), computer simulations, including QM/MM simulation,[101−104] indicate that dynamical effects do generally not contribute significantly to the rate-enhancement of chemical steps in enzymes versus solution; true dynamical effects on the rate are generally relatively small and similar in solvent and in enzymes.[84,94,105] That is not to say that protein dynamics are unimportant; the rates of conformational change often limit the overall rate of enzyme-catalyzed reactions, and formation of reactive conformations (via structural fluctuations) may be an important part of many reactions, something that is of interest intrinsically in understanding the nature of enzyme activity, if not of catalysis.[45,100]

The enzyme chorismate mutase has played a central role in debates on the origin of enzyme catalysis.[79,106−108] It catalyzes the Claisen arrangement of chorismate into prephenate. Importantly, the mechanism of the reaction is the same in the enzyme as in solution (e.g., it does not involve covalent bonds between the enzyme and the reacting species). QM/MM modeling of the reaction in this enzyme has, for example, validated the view that TS stabilization by the enzyme contributes significantly to the rate-enhancement of the reaction.[44,47,107,109−113] This contradicts proposals that binding a reactive conformation (sometimes described as a 'near-attack' conformation (NAC)) is all that is required for catalysis.[79] Free energy perturbation molecular dynamics studies with both QM/MM[107] and EVB[106] methods indicate that forcing the conformation of chorismate from that preferred in solution (diequatorial) into the enzyme-bound conformation (diaxial) costs 3.8−5 kcal mol^{-1}, which represents 40−55% of the difference in activation free energy between solution and the enzyme; the remainder of the barrier lowering is due to specific transition state stabilization. A recent analysis of multiple DFT QM/MM reaction pathways in the enzyme and in water indicated that the reaction pathways in these environments are subtly different, including small but significant differences in the TSs.[44] The enzyme compresses chorismate, which destabilizes the enzyme-bound substrate compared to solution; this difference is related to the high affinity of the enzyme for the TS. Importantly, comparison between the pathways calculated in the enzyme and in water accounts for catalysis by the enzyme, i.e., the lowering of the energy barrier. As was ascertained in previous work,[106,109,114] TS stabilization in the enzyme is predominantly electrostatic.

Central to recent debates on dynamics in catalysis are the large kinetic isotope effects (KIEs) found for a number of enzyme-catalyzed hydrogen transfer reactions and their often unusual temperature dependence. KIEs are found in the transfer of hydrogen (as a proton (H^+), hydride (H^-) or hydrogen atom), which is an important step in many enzyme-catalyzed reactions; when the transferring particle is replaced by a heavier isotope of hydrogen (tritium (T) or deuterium (D)), this can lead to a measurable change in reaction rate. When the KIE is large (e.g., $k_H/k_D > 7$), the reaction rates must be due in large part to quantum tunneling through the barrier.[2,115,117] Experiments have indicated unusual temperature dependencies of KIEs in some enzyme reactions dominated by tunneling.[2,117−120] This has led to suggestions that new concepts may be needed to understand enzyme catalysis, such as the controversial hypothesis that specific motions or dynamics of the enzyme ('promoting vibrations') promote H-transfer,[119] and that enzymes may have evolved for this purpose.[81] Others, however, argue that similar tunneling is observed in enzymes and equivalent nonenzymatic reference reactions, and therefore the effect is not catalytic.[93,121,122] The temperature dependence of KIEs can be accounted for (in models based on TST) by a few (e.g., two) conformations with different reactivity.[123,124] Molecular modeling and simulation of the enzyme reactions involved is important to resolve these debates, because such detailed modeling offers a means to analyze what is happening at the atomic level. Applications of QM/MM methods to model tunneling-dominated reactions in enzymes such as soybean lipoxygenase-1, dihydrofolate reductase, methylamine dehydrogenase (MADH), and aromatic amine dehydrogenase

(AADH) have been reviewed in detail (e.g., refs 19 and 94). QM, QM/MM, and EVB modeling generally have indicated that there is no direct evidence for the existence of catalytic 'promoting vibrations'.[2,7,82,83,121] QM/MM simulations of AADH and MADH indicate that subtle conformational changes in the active site can affect tunneling probability and reaction barriers.[2,87,88] For example, the presence or absence of a hydrogen bond from Thr172 to the reacting Asp128 carboxylate in AADH (Figure 2) affects which carboxylate oxygen of Asp128 is favored to receive the proton, leading to different barriers.

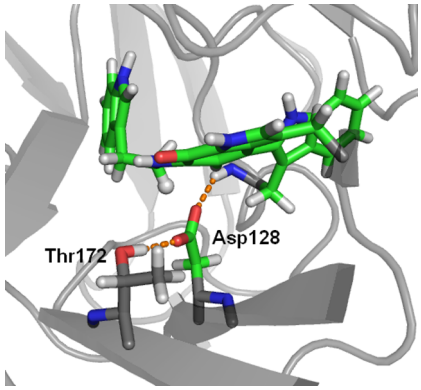

Figure 2. Tryptamine-derived iminoquinone complex (prior to the tunnelling-dominated proton transfer) in aromatic amine dehydrogenase, optimized at the B3LYP/6-31G(d)-CHARMM27 level.[87] Both Asp128 oxygens can in principle accept the hydrogen (depicted as a small sphere), but transfer to the oxygen that accepts a hydrogen bond from Thr172 is preferred.

Kanaan et al. recently studied the temperature dependence of the KIE related to hydride transfer in thymidylate synthase,[85] which converts 2′-deoxyuridine 5′-monophosphate (dUMP) into 2′-deoxythymidine 5′-monophosphate (dTMP) with the use of N5,N10-methylene-5,6,7,8-tetrahydrofolate as reductant and methylene donor. Because dTMP is needed for synthesis of DNA, the enzyme is an important drug target for cancer treatment. A hydride is transferred from tetrahydrofolate to an exocyclic methylene intermediate, resulting in dihydrofolate and dTMP. This was previously established to be the rate-limiting step in the enzyme, by experiment[125] and QM/MM modeling.[126,127] Their previous work[127] indicated that hydride transfer is concerted with the breaking of a C−S bond in the methylene intermediate (between Cys146 and the former dUMP), but the mechanism is highly asynchronous. In the recent study,[85] the antisymmetric combination of the breaking and forming bond in the hydride transfer was therefore used as a geometrical reaction coordinate to follow the reaction. First, Kanaan et al. obtained potential energy surfaces (PESs) by performing energy minimization along this coordinate. The QM region consisted of the main parts of the folate and dUMP as well as the side-chains of Cys146 and Arg164. Subsequently, free energy profiles were calculated at the AM1-CHARMM27 level by performing MD simulations along the reaction coordinate at four different temperatures for which experimental KIEs are available, with either protium (H) or tritium (T) as the hydride. Corrections for quantum vibration, recrossing of the barrier and tunneling were calculated using frequencies obtained from normal-mode analysis,[128] Grote−Hynes theory,[129,130] and the small-curvature tunneling approximation,[84,131] respectively. The phenomenological $\Delta G^{\ddagger}$ and KIE for each temperature was then obtained using ensemble average variational transition-state theory with multidimensional tunneling.[84,131] The results indicate that none of the contributions to the $\Delta G^{\ddagger}$ are temperature dependent, leading to temperature independent KIEs (in the studied range) in line with experiment. KIEs calculated from the classical barriers are smaller than the experimental ones, in line with the observation that for protium, ∼91% of the hydride transfers proceed by tunneling, which reduces the barrier by ∼1.5 kcal mol^{-1}, whereas for tritium this is ∼80% and ∼1.0 kcal mol^{-1}, respectively. The final calculated KIEs show large standard deviations, which are not necessarily only due to uncertainties in the calculation of barrier recrossing and tunneling contributions but also reflect the fluctuating protein environment. According to the authors, their simulations indicate that the enzyme serves as a 'temperature buffer', with the same thermal fluctuations coupled to the reaction (i.e., 'active site temperature') at each global temperature studied. Furthermore, movement of amino acids such as Arg166, which polarizes the C−S bond that breaks before the hydride transfer is completed, appeared to be strongly coupled to the hydride transfer. This may demonstrate how thymidylate synthase has evolved to create the optimal environment to enhance the most difficult chemical step in the overall reaction.

EXAMPLES OF QM/MM MODELING OF DRUG TARGET ENZYMES

Acetylcholinesterase and Butyrylcholinesterase. Increasingly, QM/MM methods are being applied to enzymes that are drug targets, often with the aim of providing information for drug design. An example is cholinesterases, which catalyze hydrolysis of the neurotransmitter acetylcholine (Ach), necessary for allowing cholinergic neurons to return to their resting state. Inhibitors of cholinesterases can therefore be used in treatment of diseases such as Alzheimer's and Parkinson's. There are two types of cholinesterases: acetylcholinesterase (AChE) and butyrylcholinesterase (BChE). The first has a very high catalytic efficiency for ACh hydrolysis and is mainly found in cholinergic synapses, whereas the latter (with lower efficiency) is widely distributed in tissues and plasma. Both feature a typical Ser-His-Glu catalytic triad, commonly found in serine hydrolases. Hydrolysis of ACh starts by nucleophilic attack of the serine on to the carbonyl oxygen of ACh, followed by proton transfer from the histidine and elimination of a primary alcohol, leading to an acylenzyme. Zhang et al. first studied this reaction with ab initio QM/MM methods.[132] Minimum energy paths were optimized at the HF/3-21G-AMBER ff94 QM/MM level, and single point MP2/6-31+G(d)-AMBER ff94 calculations subsequently revealed a potential energy barrier consistent with experiment (10.5 and 12 kcal mol^{-1}, respectively). The glutamate (Glu334) was found to provide electrostatic stabilization of the TS and the acyl-enzyme, in agreement with previous modeling studies[133] (and without the need for previously proposed catalytic 'low-barrrier' hydrogen bonds or 'charge-relay' mechanisms). Recently, Zhou et al. calculated free energy profiles of both reaction steps, using B3LYP/6-31G(d)-AMBER ff99SB MD simulations.[56] In the acylation step, a short hydrogen bond was found between His447 and Glu334, and the simulations indicated spontaneous transfer between these species. The subsequently determined barrier for proton transfer was indeed low (∼2 kcal mol^{-1}), but the proton was never observed to

dx.doi.org/10.1021/bi400215w | Biochemistry 2013, 52, 2708−2728

remain in between the residues and proton-localization on His447 was favored. This is in line with previous QM/MM and EVB studies on serine hydrolases, which concluded that a 'low-barrier' hydrogen bond is not involved in catalysis.[134−136] For the deacylation step, it was shown that Glu202 (located close to the catalytic triad) is favored to be protonated, in agreement with previous modeling studies.[137] The barrier for deacylation was calculated to be higher than that for acylation, as expected from experiment[138] and also in line with QM/MM potential energy calculations using a more limited computational protocol (e.g., without polarization of the QM region by the MM region).[139] Chen et al. recently also reported QM/MM-FE free energy profiles at the MP2/6-31+G(d)-AMBER level for acylation and deacylation of ACh in BChE.[140] Despite the similarity of the AChE and BChE structures and active sites, acylation was found to be rate-determining in this case (with a free energy barrier that agreed very well with experiment). The authors suggested that this can explain kinetic data that indicate a difference between the rates of ACh and acetyl*thio*choline hydrolysis by BChE[141] (but not by AChE).[138] A subsequent QM/MM-FE study on acetylthiocholine hydrolysis by BChE confirmed that acylation is indeed rate-limiting for this reaction and also demonstrated that the presence of an additional substrate molecule in a peripheral anionic site can explain the experimentally observed substrate activation effect.[142]

QM/MM simulations have also been applied to obtain insight into enzyme−inhibitor interactions in AChE. A very high affinity inhibitor of AChE, *syn*-TZ2PA6, can be made from its precursor fragments by a 1,3-dipolar cycloaddition reaction between the azide and acetylene moieties.[143] In solution, this reaction results in equal amounts of *syn*-TZ2PA6 and *anti*-TZ2PA6, the latter of which has lower affinity. However, *in situ* production of *syn*-TZ2PA6 only is observed when the precursors were added to AChE. Senapati et al.[144] first calculated MEPs at the B3LYP/6-31G(d)-AMBER ff94 QM/MM level for both reactions based on the AChE-product complexes obtained by crystallography. This indicated that the azide and acetylene moieties need to lie parallel in order to form the *syn* complex, and antiparallel to form the anti complex. Conventional and targeted MD simulations of the reactant complexes indicated that the enzyme enforces the parallel orientation of the precursors, thereby explaining its selective production of the high-affinity *syn*-TZ2PA6 inhibitor. The same group also reported QM/MM-FE and MD studies that explained how, unexpectedly, the binding of a positively charged trifluoroacetophenone inhibitor could still lead to an acyl-enzyme after mutation of the catalytic triad His447.[145] Apart from these reversible inhibitors, which are drug-leads for treatment of disease, irreversible inhibitors of AChE are also known: these are highly neurotoxic compounds that attach a phosphorus to the catalytic serine, such as the nerve agents sarin and tabun and the insecticide paraoxon. Liu et al. modeled the dephosphorylation (reactivation) mechanism of paraoxon-methyl (dimethylphosphoryl) with AChE in detail, using QM/MM-FE calculations based on MEP optimization at the B3LYP/6-31G(d)-AMBER level.[146] QM/MM calculations have also been used to obtain insight in the reaction mechanisms of AChE with the nerve agents tabun[147] and sarin,[148] and such insights may help in development of treatments against poisoning. Finally, BChE is the primary enzyme breaking down the widely abused drug cocaine into inactive metabolites; QM/MM modeling has been used to help design variants with higher catalytic activity, as discussed below in the section Computer-Aided Enzyme Design.

Fatty-Acid Amide Hydrolase. Fatty-acid amide hydrolase (FAAH) is involved in the degradation of biologically relevant fatty acid amides (including the endocannabinoid anandamide) and is a promising target for the treatment of anxiety, pain, and hypertension.[149] It contains an unusual Ser-Ser-Lys catalytic triad, the function of which was elucidated by QM/MM reaction modeling.[150] B3LYP/6-31+G(d) corrected PM3-CHARMM27 potential energy surfaces, leading to a activation barrier consistent with experiment for the reaction of oleamide, indicated that the neutral Lys142 deprotonates the nucleophilic Ser241 via Ser217, which acts as a proton shuttle. QM/MM-FE Monte Carlo simulations by another group, using PDDG/PM3 as the QM method, also support this mechanism and, furthermore, reproduce the influence of the Lys142Ala mutant on the rate of hydrolysis on different substrates.[151] QM/MM and MD simulations further highlighted interesting conformational effects in FAAH: the acylation of oleamide occurs via a high-energy conformational substate of the enzyme−substrate complex.[45,152] Subsequently, QM/MM reaction modeling offered direct insight into the possible binding modes of carbamic acid aryl ester lead compounds,[153] which could not be distinguished based on docking or quantitative structure−activity relationship (QSAR) approaches.[154] This knowledge was subsequently used in the design of inhibitors with increased potency.[155] The binding mode predicted by QM/MM modeling was later confirmed by crystallography.[156] QM/MM modeling of the reactions of three carbamate compounds provided further insight.[157] Michaelis complexes were built based on the previously determined preferred binding modes and equilibrated using MM (CHARMM27) MD. Subsequently, QM/MM minimization of structures along geometrical reaction coordinates describing the mechanism was performed at the PM3-CHARMM27 level, to generate potential energy profiles for the whole reaction. The first reaction step was modeled using two reaction coordinates (creating a 2D PES), one describing proton abstraction from Ser241 by Ser217 together with nucleophilic attack by Ser241 and the other describing the proton transfer between Ser217 and Lys142. Energies for approximate TS and intermediate structures were then calculated at the B3LYP/6-31+G(d)-CHARMM27 level and[150] showed that the rate of the inhibiting carbamylation of Ser241 is determined by the formation of the first tetrahedral intermediate in all three cases.[157] The key TS of the reaction is not significantly affected by electron-donating substituents on the inhibitors (because it is dominated by the proton transfer between Ser241 and Ser217, see Figure 3), providing an explanation for the observation that these substituents do not affect inhibitor potency *in vivo*, whereas they do affect the intrinsic reactivity.[154] This knowledge can be used in the design of lead compounds with improved potency *and* selectivity. Together, these studies on FAAH inhibitors exemplify how QM/MM reaction modeling can contribute directly to rational drug design for an important drug target.

HIV-1 Protease. Human immunodeficiency virus type 1 (HIV-1) causes the acquired immunodeficiency syndrome (AIDS), which is still one of the most serious health problems in the world. Three enzymes are essential for replication of HIV-1 and can thus be targeted by anti-AIDS drugs: reverse transcriptase, protease, and integrase. All three enzymes have been studied using QM/MM modeling, offering detailed pictures of their reaction mechanisms.[158−162] HIV-1 protease,

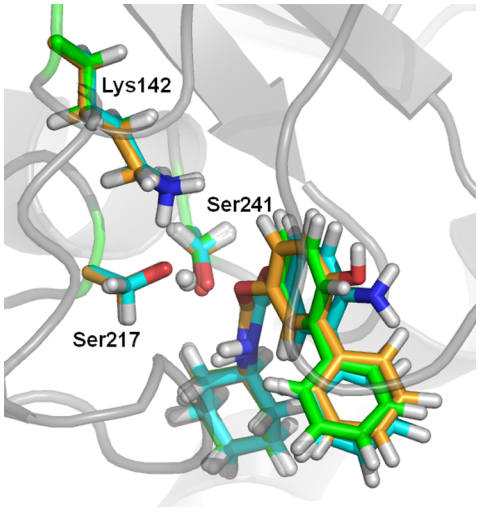

Figure 3. Transition state structures (from B3LYP/6-31+G(d)//PM3-CHARMM27 modeling) for the formation of covalent enzyme–inhibitor complexes in fatty acid amide hydrolase, with three different carbamate compounds (in green, cyan, and orange).[157] The TSs are very similar and are dominated by deprotonation of Ser241.

an aspartic protease which cleaves the peptide bond between Phe/Tyr and Pro, has been the main target for anti-AIDS drug therapy. The homodimeric enzyme features two aspartic acid residues that form a so-called aspartyl-dyad, Asp25/25′ (one from each dimer). It has now been established that the reaction proceeds by nucleophilic attack of a water molecule (placed near the aspartyl-dyad) on the peptide carbonyl carbon (concerted with proton transfer to one of the aspartates), followed by protonation of the peptide nitrogen (from the aspartate that received the proton in the first step). The nature of the intermediate between these two steps, however, is still debated: it is probably either a gem-diol[158] or an oxyanion.[163] This issue is relevant for drug design, because the enzyme is expected to show high affinity toward analogues of the intermediate. Carnevale et al.[161] used QM/MM (BLYP-AMBER ff94) and QM only (B3LYP) calculations to argue that the gem-diol intermediate is much more stable than the anionic intermediate. This conclusion is in line with subsequent X-ray structures[164] and was recently further confirmed by a QM study on a large part of the enzyme active site, which included an extensive comparison of QM methods for description of the HIV-1 protease reaction.[165] It must be noted, however, that these studies did not include comprehensive conformational sampling, and thus no final conclusion about the nature of the intermediate can be drawn.

QM/MM simulation has been used extensively to study HIV-1 protease/inhibitor interactions (see also ref 19). For example, Suresh et al.[166] used the subtractive ONIOM method at the B3LYP/6-31G(d)-AMBER level to investigate the role of a conserved water molecule (W301) in six enzyme–inhibitor complexes. W301 forms four hydrogen bonds to bridge the Ile50/50′ NH groups in the active site cleft opposite from the aspartyl-diad (the so-called flaps) and the CO groups at positions P2 and P′1 of the inhibitor. The approved inhibitor tipranavir is designed to replace W301. AM1-CHARMM27 MD simulations indicated that the potency of tipranavir can indeed be attributed to interactions with both Asp25/25′ and Ile50/50′,[167] and the authors suggested that introduction of a hydrogen bond donor to interact with Asp30 would lead to a more potent inhibitor. Garrec et al. recently used QM/MM Car–Parrinello MD modeling to investigate a new class of HIV-1 protease inhibitors, based on the presence of a noncovalently interacting tertiary amine and carbonyl, the so-called N···CO bond.[168] The idea behind these amino-aldehyde peptide inhibitors is to replace the hydroxyl group, present in the natural peptide substrates as well as many current inhibitors, with a group that is a better TS analogue, providing a stronger interaction with the aspartyl-dyad.[169] By considering an amino-aldehyde peptide bound to the enzyme in all possible protonation states of the aspartyl-dyad, they asserted that N···CO bond formation competes with the W301 hydrogen bond network: the two cannot coexist, which can explain the relatively poor inhibition of amino-aldehyde peptides. The simulations also indicated, however, that hydrogen bond formation between N···CO and the aspartyl-dyad is feasible, and the authors conclude that designing N···CO containing inhibitors that can replace W301 is a promising strategy. Finally, a recent study demonstrates the complementarity of QM/MM modeling, docking, and experimental methods in the analysis of another new class HIV-1 protease inhibitors.[170] Pentacycloundecane (PCU) lactam-peptide compounds with nanomolar activity against HIV protease were synthesized, and NMR techniques and QM/MM (AM1-MM) MD simulations were used to assert that effective inhibition was related to the chirality of the PCU group and its influence on the conformation of the attached peptide chain. A unique binding mode for these inhibitors was found by docking and AM1-MM MD simulations of the enzyme–inhibitor complexes, rationalizing the experimentally observed inhibition of the different compounds.

MECHANISM AND SPECIFICITY OF DRUG-METABOLIZING ENZYMES

Cytochrome P450 enzymes (P450s) are well-known for their role in drug metabolism. They catalyze a variety of reactions (e.g., hydroxylation and oxidation) for a very wide range of compounds. As well as affecting the bioavailability of drugs, they are often the cause of unwanted drug–drug interactions and variation in drug metabolism between individuals. Understanding the reactivity and selectivity of the different P450 enzymes is therefore of great pharmaceutical interest. QM calculations have been essential in elucidating fundamental details of P450 reactions.[171] For questions of specificity, large models including significant portions of the protein are often required, and QM/MM methods are particularly important in this respect. The complex electronic structure of the heme group and species involved in reaction, such as Compound I (a high-valent Fe(IV) oxo state of the heme, see e.g., Figure 9 in ref 172), can be treated using reliable QM methods (e.g., B3LYP) while the enzyme environment is treated MM.[39,172] Inclusion of the latter can be important to reveal potential differences between isoenzymes. Compound I (Cpd I) is important for the reactivity of P450s. In contrast to suggestions that other states may also be involved in certain oxidations, QM/MM studies consistently indicate that Cpd I has the highest reactivity.[173,174] Bathelt et al. studied this species in three important human P450s (2C9, 2D6, and 3A4), together with the drugs ibuprofen and diclofenac.[175] The electronic structure did not vary significantly between the species and was insensitive to the presence or absence of a substrate (as well as the QM region and the enzyme–substrate conformation). This indicates that the large differences in substrate selectivity

between P450 isoforms are not related to differences in reactivity of their Cpd I species, but rather to differences in substrate interactions in the active site (that can influence binding orientation, for example). Fishelovitch et al. studied Cpd I in P450 3A4 with no, one, or two molecules of diazepam bound.[176] With no or one diazepam molecules present, Cpd I could form hydrogen bonds that may lead to the destruction of the reactive species, whereas binding of two molecules prevented this. These results can help explain the unusual kinetics often observed for 3A4.[177] These authors also argued that Cpd I may be different in 3A4 compared to other P450 isoforms, in contrast to the results obtained by Bathelt et al.[175,178] To investigate whether the different protein environments in different P450 isoforms can influence Cpd I reactivity or not, Lonsdale et al. recently performed a comprehensive analysis of different Cpd I-enzyme conformations.[179] They first performed 5 ns MM (CHARMM27) MD simulations for the human P450 isoforms 2C9, 2D6, and 3A4 and the bacterial $P450_{cam}$, both in the presence and absence of substrates. From each of the MD simulations, 26 conformations were optimized with a QM/MM method, using B3LYP and the LACVP and 6-31G(d) basis sets for the iron and all other atoms in the QM region, respectively. The results demonstrate that the electronic structure of Cpd I varies significantly more between different conformations for any individual human isoform than between isoforms (Figure 4). Cpd I in the bacterial $P450_{cam}$ did differ from the human isoforms, displaying a significant decrease in spin density on the sulfur (accompanied by increased density on the porphyrin ring). The reactivity of Cpd I was estimated using an approximation of the Fe−O bond enthalpy, and differences between the isoforms were again not significant (smaller than the variation in different conformations, Figure 4A). This conclusion is important, as it indicates that Cpd I reactivity is essentially identical between (human) isoforms, an assumption often used in high-throughput prediction of drug metabolites. In the presence of substrates, the reactivity of Cpd I increases somewhat. This difference was argued to be due to the substrate restricting the number of water molecules that are able to hydrogen bond to the ferryl Cpd I oxygen. The spin density of the oxygen thereby increases, which in turn affects the Fe−O bond enthalpy, related to reactivity.

QM/MM methods have also been applied to model oxidation reactions in P450 enzymes. For example, Bathelt et al. studied the hydroxylation of benzene in P450 2C9. Similar barriers indicated that oxidation of benzene in a side-on or face-on approach to Cpd I may be competitive (in contrast to QM model calculations). Further, the side-on pathway appeared to favor an epoxide product, whereas the face-on pathway could lead to both epoxide and ketone products. The results indicate that aromatic hydroxylation by P450s can involve several different pathways. Oxidation reactions have also been modeled extensively in $P450_{cam}$,[180−185] the first P450 to have crystal structures available. Recently, Lonsdale et al. studied the chemoselectivity of $P450_{cam}$ toward hydroxylation or epoxidation of cyclohexene and propene.[180] The difference in activation energies, based on Boltzmann-weighted averaging of multiple QM/MM pathways, indicates that P450 chemoselectivity can be predicted by considering Cpd I reactivity, within the range of errors for the employed QM/MM methods. Nevertheless, the calculations predicted hydroxylation to be favored in both cases, whereas this is not found by experiment. A subsequent study showed that the use of dispersion-corrected B3LYP (B3LYP-D) improves the accuracy significantly,[30] now

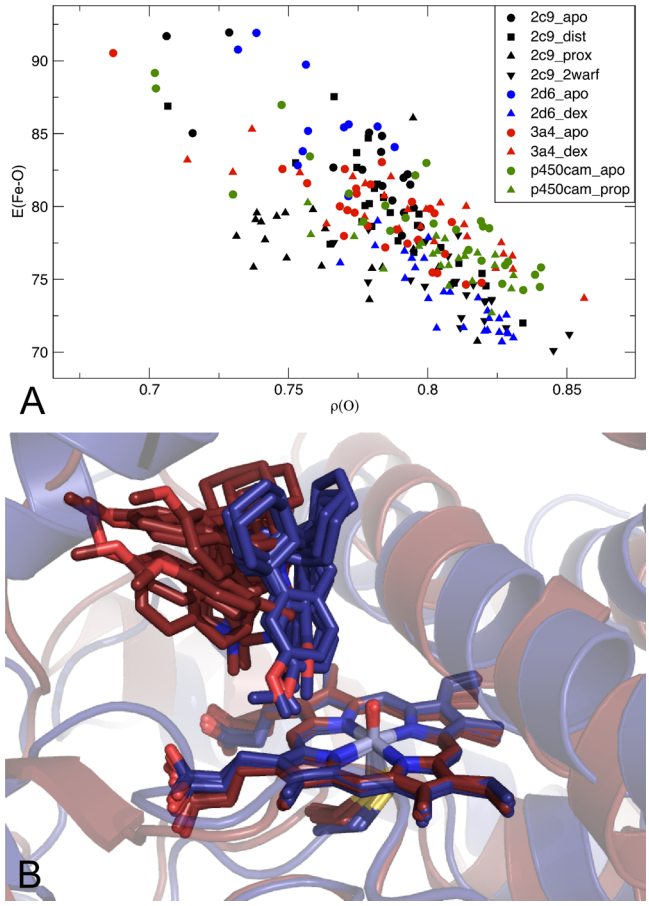

Figure 4. (A) Fe−O bond enthalpy, E(Fe−O) [kcal mol^{-1}] plotted versus Cpd I ferryl oxygen spin density (ρ(O)) for multiple structures for different cytochrome P450 isoforms, in the absence (circles) or presence (triangles, squares) of ligands (isoforms indicated by different colors as shown in the legend; reproduced from ref 179). (B) Examples of structures of Cpd I with dextromethorphan in 2D6 (blue) and 3A4 (red) obtained from MM molecular dynamics simulation and subsequent QM/MM (B3LYP/6-31G(d)-CHARMM27, with LACVP basis for Fe) optimization.[179]

yielding the correct chemoselectivity for propene oxidation. This result demonstrates again the importance of testing QM(/MM) methods for the task at hand, as well as the potential for QM/MM modeling to predict chemoselectivity in P450s. Recently, Oláh et al. showed how QM/MM reaction modeling can be used for the prediction of pharmaceutically relevant P450 enzyme metabolites.[186] They investigated two different metabolic routes of dextromethorphan in P450 2D6 (Figure 4B): aromatic hydroxylation and O-demethylation. Although the former is a major route for other compounds with methoxyaromatic rings, it is not observed experimentally in 2D6. Gas phase QM calculations of Cpd I and the model substrate anisole, using B3LYP/LACVP** for geometry optimization and B3LYP with the LACV3P basis on iron and the 6-311++G(d,p) basis on other atoms for energy calculation, suggested that the two reactions can occur competitively. Enzyme−substrate models were built by placing the substrate in five different positions, and both stereoisomers of N-protonated dextromethorphan were considered. Subsequently, the system was solvated and truncated to 25 Å around the heme iron, and after the system was heated to 300 K, 2 ns of MM (CHARMM27) MD was performed. The simulations

dx.doi.org/10.1021/bi400215w | *Biochemistry* 2013, 52, 2708−2728

indicated that a pose with a salt-bridge to Glu216 was most stable. Both putative reactive sites could readily approach the reactive Cpd I oxygen, so MD simulation alone cannot explain the lack of aromatic hydroxylation found experimentally. For both aromatic hydroxylation and O-demethylation, three favorable conformations were selected from the MD simulation to perform QM/MM reaction modeling employing the same QM method and basis as the gas phase calculations. After MM minimization, the system was optimized with heme and the aromatic ring (incl. O-methyl) of dextromethorphan treated QM. Potential energy profiles (for each snapshot) were obtained along the distance between the ferryl oxygen and the abstracted hydrogen atom or the aromatic carbon. Calculated energies (including zero-point energy corrections from the QM calculations) indicate a strong preference for O-demethylation (by >12 kcal mol^{-1}), consistent with experiment. This preference arises because interactions between dextromethorphan and the enzyme prevent the formation of the preferred TS conformation for aromatic hydroxylation.

In addition to the above applications, QM/MM methods have been applied to the metabolism of nicotine by P450 2A6 (providing insights that might help in the design of smoking cessation drugs),[187] the selectivity for hydroxylation or desaturation of alkanes by $P450_{cam}$[188] and the deactivation of P450 2B4 by a single mutation.[189]

After initial metabolism by CYP450s or other enzymes, many drug metabolites need to undergo a conjugation reaction before they can be eliminated. Enzymes catalyzing these so-called phase II reactions include methyltransferases, sulfotransferases, epoxide hydrolases, and glutathione *S*-transferases. QM/MM reaction modeling has been used to provide insight into the mechanisms of these enzymes (see, e.g., refs 48, 190−193) Of particular importance to understanding individual differences in drug metabolism is the influence of polymorphisms on the catalytic efficiency for different substrates. Bowman et al. modeled conjugation of glutathione with 1-chloro-2,4-dinitrobenzene (CDNB) by wild-type and active site mutants of M1-1 glutatione *S*-transferase (GST),[23] a reaction often used as an activity assay for GSTs. The reaction involves significant changes in solvation, emphasizing the need for QM/MM dynamics simulations.[193] To combine computational efficiency with accuracy, specifically parametrized AM1 was used as the QM method. Overall, the results agreed well with experiment. For the wild-type enzyme, a very low activation barrier (∼1 kcal mol^{-1}) for glutathione conjugation was found, in line with the expectation that product release is rate-limiting. The Tyr6Phe mutation increased the barrier of the formation of the initial Meisenheimer-complex (an unstable tetrahedral-intermediate) to ∼4 kcal mol^{-1}, but did not alter the energetics of the subsequent elimination of chloride. This implies that Tyr6 mostly serves to reduce the pK_a of the enzyme-bound glutathione thiolate. The Met108Ala mutation did not alter the reaction profile compared to the wild-type, confirming that Met108 is important for binding of CDNB, but not for catalysis. The reaction profile for Tyr116Phe GST was also very similar to wild-type, in line with experiments that suggest that a slight increase in activity toward CDNB for this mutant is due to product release. In contrast, the mutation has decreased activity toward phenanthrene 9,10-oxide, which was previously modeled successfully with similar QM/MM methods.[193] QM/MM modeling has also been used to investigate the catalytic mechanism of glutathione *S*-transferase A3-3[194] and the irreversible inhibition of glutathione *S*-transferase P1-1 (which is overexpressed in certain cancers) by the cancer-drug ethacraplatin.[195] Further, a recent QM/MM study revealed in detail the determinants of regio- and enantioselectivity for nucleophilic ring-opening in two substrates by soluble epoxide hydrolase;[48] understanding the determinants of selectivity in epoxide ring-opening may help in the design of biocatalysts for synthesis of enantiopure compounds.

UNDERSTANDING DRUG RESISTANCE

The emergence and spread of drug resistance in pathogenic bacteria and viruses is a major problem for public health. β-Lactamases are the main family of enzymes responsible for antibiotic resistance in pathogenic bacteria. They can be divided into four classes: classes A, C, and D are serine β-lactamases, and class B enzymes are metallo-β-lactamases (MBLs). The enzymes break open the β-lactam ring, present in most clinically used antibiotics, and then release the inactive product. Detailed understanding of the enzyme mechanisms may help the design of inhibitors for these enzymes and new antibiotics. The TEM enzymes are the archetypal class A β-lactamases and are extremely widespread in Gram-negative bacteria such as *Escherichia coli* and *Klebsiella pneumoniae*. Hermann et al. studied the acylation step of benzylpenicillin in TEM-1[196,197] and subsequently also the deacylation step with QM/MM methods.[198] They obtained potential energy surfaces by AM1-CHARMM27 optimizations corrected by single point B3LYP/6-31G(d) calculations. The mechanism for deacylation, reasonably well established experimentally, was confirmed, with Glu166 acting as the base. The mechanism for the rate-limiting acylation step, however, was previously not well established. The studies by Hermann et al. indicated that the mechanism with Glu166 abstracting the proton from Ser70 (which subsequently attacks the β-lactam ring) via a conserved water molecule was feasible. Lys73 was found to stabilize the TS of acylation and to act as a proton shuttle in the subsequent steps. Meroueh et al.[199] used the subtractive ONIOM method to calculate pathways for acylation of TEM-1 with penicillic acid, using optimization at the HF/3-21G-OPLS-AA level and energy calculation at the MP2/6-31+G(d)-OPLSA-AA level. They concluded that both Lys73 and Glu166 could act as the base, with Lys73 somewhat favored. They suggested that the alternative mechanisms could be competitive and that serine β-lactamases may use different pathways for different substrates. Because of the relatively low levels used in QM/MM optimization in both studies, and limited consideration of conformational effects, the conclusions are not certain. More recently, however, the pathway with Glu166 acting as a base was recalculated for benzylpenicillin in TEM-1 using high-level QM/MM methods,[200] employing B3LYP/6-31+G(d) for QM/MM optimization and up to SCS-MP2/aug-cc-pVTZ for QM/MM energy calculations (Figure 5). It was confirmed that proton abstraction from Ser70 is concerted with the nucleophilic attack of Ser70 on the β-lactam ring. The highest level of theory indicates a barrier of 4.1 kcal mol^{-1} for this probable rate-limiting step, somewhat low compared to experiment, but reasonable considering that multiple enzyme−substrate conformations and entropy effects were not included. Importantly, this result strongly supports the mechanism with Glu166 acting as a base, which is further supported by recent neutron-diffraction experiments.[201]

Gherman et al.[202] studied the deacylation of cephalothin from the class C β-lactamase P99 and a penicillin binding protein (PBP), which is a target for β-lactam antibiotics.

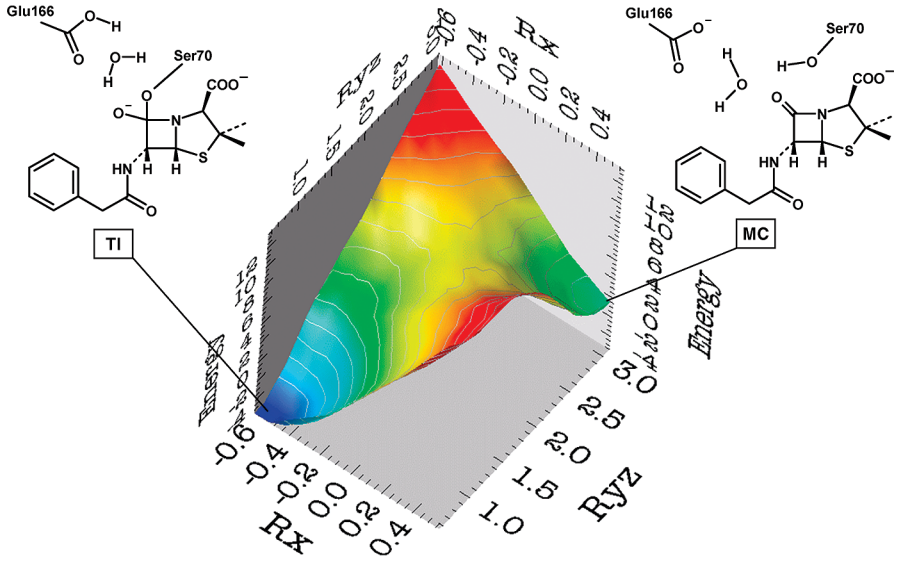

Figure 5. Potential energy surface of tetrahedral intermediate (TI) formation in the acylation step of the class A β-lactamase TEM-1 with benzylpenicillin, calculated at the B3LYP/6-31G+(d)-CHARMM27 level.[200] Rx describes the proton transfer from the water molecule to Glu166, and Ryz describes both the proton transfer from Ser70 to the water molecule and the nucleophilic attack on the β-lactam carbonyl group. Figure reproduced from ref 200. Copyright 2009 American Chemical Society.

B3LYP/6-31G(d)-OPLS-AA optimizations were performed for the acyl-enzymes and some deacylation TSs with different protonation states of the relevant residues. Free energies of activation were estimated using vibrational analysis, which indicate that deacylation is efficient in P99 and inefficient in PBP, as expected. For P99, a pathway with Tyr150 acting as the base is supported, with the hydroxyl proton transferred to an unprotonated Lys67 in a concerted fashion. For PBP, it was suggested that the equivalent Lys (Lys65) could act as the base, whereas the equivalent Tyr (Tyr159) cannot. The difference between P99 and PBP was found to be the more favorable electrostatic environment of Tyr150 in P99, which includes an important interaction with Lys315. More recently, the covalent inhibition of PBP 2a with the β-lactams methicilin and nitrocefin was studied with the ONIOM QM/MM approach,[203] and Carr-Parinello QM/MM molecular dynamics studies were employed to obtain insight into the active-site protonation states of the class C β-lactamase 908R in the absence and presence of cephalothin.[204] It is important to stress here that for β-lactamases, as for many other enzymes, conformational sampling (e.g., in molecular dynamics simulations) may be essential for understanding and modeling activity.[205]

Although metallo-β-lactamases (MBLs) are still relatively rare, they do form a significant threat due to their rapid evolution and spread across species as well as the difficulty of finding general inhibitors.[206] MBLs can be subdivided into enzymes active with either one or two Zn^{2+} bound (class B1), those active only with one Zn^{2+} bound (B2) and those active only with two Zn^{2+} bound (B3). For dizinc MBLs, it is believed that the hydrolysis of the β-lactam ring starts by the nucleophilic attack of a zinc-bound hydroxide on the β-lactam carbonyl, followed by the cleavage of the C−N bond. The latter could either be assisted by protonation of the nitrogen or by stabilization of the second zinc ion when present. The nature of the proton donor is still debated. Dal Peraro et al. used QM/MM Car−Parrinello MD at the BLYP-AMBER ff94 level to study the hydrolysis of cefotaxime in the B1 MBL BcII, with one Zn^{2+} bound.[207] A series of short MD simulations followed the nucleophilic attack of a zinc-bound hydroxide and showed that a water molecule enters the solvation sphere of the zinc. They suggest that this water molecule can subsequently serve as the proton donor, regenerating the zinc-bound hydroxide. Later, they also modeled the hydrolysis of cefotaxime in the B1 MBL CcrA, which has two Zn^{2+}, with similar methods.[208] Essentially the same pathway was proposed, but now with nucleophilic attack and proton transfer to the nitrogen concerted.

It is important to note, however, that the enzyme−substrate complex used by Dal Peraro et al.[207,208] is questionable: the carboxylate moiety on the substrate was assumed to interact with the zinc ions through a water molecule, whereas protein crystallography indicates a direct interaction.[209] This binding mode was further verified by QM/MM studies[210] and subsequently used for the modeling of moxalactam hydrolysis in the dizinc B3 MBL L1.[211] SCC-DFTB-CHARMM27 modeling of the ring-opening was performed by following the nucleophilic attack of the hydroxide and the C−N bond cleavage in one reaction coordinate and a proton transfer from the (former) hydroxide to Asp120 in another. The resulting 2D minimal energy surface showed that the reaction is essentially stepwise, starting with a rate-limiting nucleophilic attack and C−N bond cleavage, followed by an almost spontaneous protonation of Asp120. On the basis of the optimized geometries, a free energy profile was obtained using SCC-DFTB-CHARMM27 MD simulations and subsequent energy corrections using single-point B3LYP-CHARMM27 calculations (with LANL2DZ for zinc and sulfur and 6-31G(d) for all other atoms as basis sets). The barrier is in line with experiment (23.5 vs 18.5 kcal mol^{-1}, respectively) and indicates that a reasonably stable intermediate is formed, in which the newly formed carboxylate is stabilized by one Zn^{2+} and the (unprotonated) nitrogen leaving group by the other. Xu et al. also studied the interaction and hydrolysis of biapenem with the monozinc class B2 MBL CphA using QM/MM methods.[212−214] On the basis of a crystal structure of an

enzyme-intermediate complex of CphA with a biapenem,[215] they first investigated the enzyme−substrate complex using SCC-DFTB-CHARMM27 MD simulations,[212] confirming that the Zn^{2+} was coordinated by the substrate carboxylate, Cys221, His263, and Asp120. Importantly, a crystallographically observed water was found to from stable interactions with the β-lactam carbonyl and Asp120. Subsequent reaction modeling at the SCC-DFTB-CHARMM27 level (validated by single-point B3LYP-CHARMM27 and small model B3LYP calculations) indicated that the reaction proceeds via a concerted S_N2-like mechanism, with the water attacking the carbonyl carbon, cleavage of the C−N bond, and Asp120 accepting the remaining proton from the nucleophilic water. They also considered His118 as the base instead of Asp120, as originally suggested,[215] but found it not to be competitive. More recently, the full reaction of biapenem with CphA was also modeled at the SCC-DFTB-CHARMM27 level.[214] This indicated that Asp120 donates the proton it obtained from the nucleophilic water to the former β-lactam nitrogen. As expected, the initial S_N2-like nucleophilic addition and elimination was found to be rate-limiting. Interestingly, this work further identified the crystallographically observed enzyme-intermediate complex as belonging to a minor pathway, in contrast to the original suggestion.[215] A recent QM/MM (B3LYP/LACVP*-OPLS-AA) and MM metadynamics study supports the mechanism for biapenem hydrolysis in CphA obtained by Wu et al.[214] and further indicates that the bicyclic derivative of biapenem has significant affinity for B2 MBLs, highlighting the potential of designing inhibitors based on this derivative.[216] Overall, these studies on MBLs demonstrate the mutual benefit between protein crystallography and QM/MM modeling. On the one hand, high-resolution experimental data on the enzyme−substrate complex is required to set up reliable models for QM/MM calculations. On the other hand, QM/MM modeling can verify or help modify mechanistic proposals.

■ COMPUTER-AIDED ENZYME DESIGN

The remarkable rate-enhancements achieved by enzymes have inspired scientists to develop methods to design enzymes for specific industrial or medical applications. Computer modeling, and QM/MM reaction modeling in particular, can assist in the rational design of enzymes by understanding the factors that affect catalysis and potentially predict mutations that enhance activity.[42,217] Martí and co-workers have demonstrated the use of QM/MM reaction modeling to design alternative catalysts for the chorismate to prephenate rearrangement,[218,219] a reaction normally catalyzed by chorismate mutase (see section "Investigating Principles of Enzyme Catalysis"). First, they compared AM1-CHARMM27 QM/MM free energy profiles for the reaction in aqueous solution, chorismate mutase (from *Bacillus subtilis* and *E. coli*) and the synthetic catalytic antibody 1F7.[218] The obtained differences in the barriers agreed well with experimental data. Comparison of TS binding in the natural enzymes and 1F7 indicated that the interactions of the carboxylate groups in the reacting species with 1F7 were far from optimal. By making a single mutation, they improved the TS interactions with the binding site. The computed barrier for the mutant 1F7 was 4.5 kcal mol^{-1} lower than the original, only 2.4 kcal mol^{-1} above the most efficient enzyme. Subsequently, they turned to isochorimsate pyruvate lyase (IPL),[219] which catalyzes the conversion of isochorismate into pyruvate but also shows activity for the chorismate to prephanate reaction. After a free energy profile was obtained that illustrated the moderate catalysis of IPL, the simulations at stages during the reaction were analyzed. This revealed that the diaxial conformation of chorismate, important for formation of the TS, is not retained in the active site of IPL. Comparison with natural chorismate mutases indicated that this could be attributed to the lack of a bulky residue at position 38 (35 in *E. coli* chorismate mutase). The Ala38Ile mutation was therefore proposed, and reaction modeling confirmed that this mutation helps constrain chorismate in the diaxial position. Furthermore, the calculated free energy barrier of the mutant IPL showed a decrease of 4.4 kcal mol^{-1} compared to the wild-type. The work of Mayo et al. on *E. coli* chorismate mutase corroborates the influence of the proposed mutation: a bulkier residue at 35, introduced by the Val35Ile mutation, increases the rate for the reaction (by a factor of 2), whereas the Val35Ala mutation reduces the rate.[220] Further calculations indicated that the Ala38Ile mutation may also somewhat improve the catalytic efficiency of IPL for its natural reaction.[221]

Zhan et al. have provided a prime example of how such computationally obtained insights can complement experimental techniques in the optimization of an enzyme to catalyze a reaction of biomedical relevance:[222−225] the detoxification of cocaine by butyrylcholineesterase (BChE, see section "Examples of QM/MM Modeling of Drug Target Enzymes" above). The primary pathway for cocaine metabolism is hydrolysis by BChE, but this reaction is not very efficient. BChE mutants with a higher catalytic activity against (−)-cocaine (the active enantiomer) can be designed, offering an attractive "protein-drug" for treatment of cocaine abuse and dependence. The mechanism is essentially the same as ester hydrolysis catalyzed by other serine hydrolases, involving enzyme acylation and deacylation. Four steps can be distinguished: (1) nucleophilic attack of Ser198 on the ester carbon to form a tetrahedral intermediate (TI), (2) proton uptake from His438 by the leaving alcohol group, (3) nucleophilic attack of a water molecule (assisted by proton transfer to His438) to form another TI, and (4) breakdown of the TI with the carboxylic acid leaving and the enzyme returning to its resting state. Zhan and Gao first studied these steps in BChE using the ONIOM method,[226] with geometries optimized at the HF/3-21G-AMBER level and energies calculated at the MP2/6-31G(d)-AMBER level. The substrate, catalytic triad (S198, H438, and E325) and oxyanion hole (formed by the backbone of G116, G117, and A199) were treated QM. The first and third steps were calculated to have similar energy barriers, with the latter just higher (13.0 vs 14.2 kcal mol^{-1}). The barrier for the first step was ~3.7 kcal mol^{-1} higher than that for hydrolysis of ACh by AChE calculated using QM/MM methods at a similar level,[131] and the authors attributed the difference to the fact that only two of the three possible hydrogen bonds in the oxyanion hole were formed in the TSs for cocaine hydrolysis in BChE. Subsequently, MM MD simulations of the TS for the first step were used to propose mutations to improve interactions between the TS carbonyl oxygen of (−)-cocaine and BChE,[227] starting from the A328W/Y332A mutant previously designed to improve reactivity.[228] The simulations indicated that the A199S/S287G/A328W/Y332G mutant would significantly increase effective hydrogen bonding to the TS. Kinetic measurements showed that this mutant is indeed much more efficient than the previous mutant: catalytic efficiency improved ~456-fold (instead of ~9-fold with A328W/Y332A BChE) over WT BChE. Similar work indicated that the A199S/F227A/A328W/Y332G mutant had a ~151-

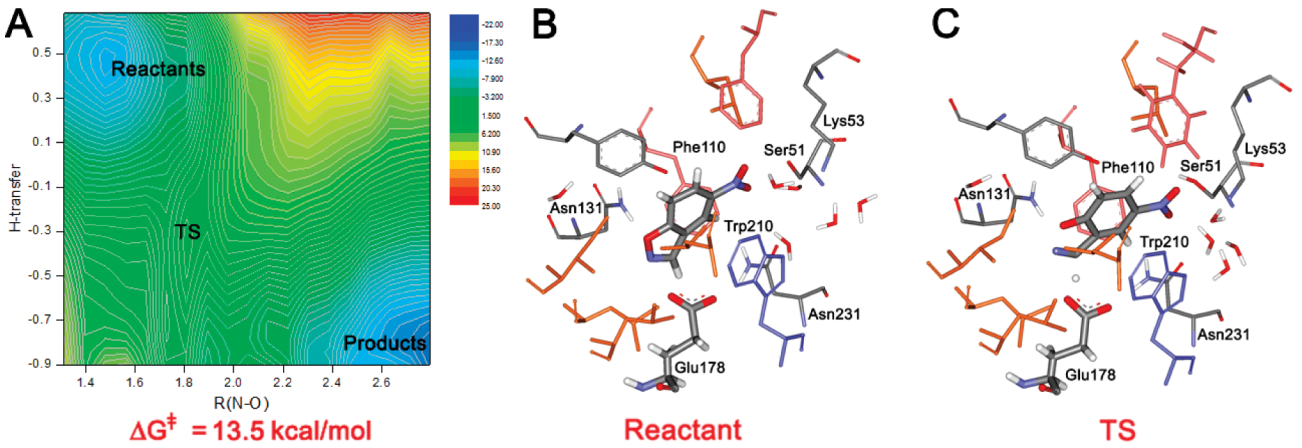

Figure 6. (A) Free-energy surface for Kemp elimination in the designed enzyme KE10(V131N), obtained by QM/MM-FE calculations at the PDDG/PM3-OPLS-AA level.[230] (B) Configuration of the reactant state at the end of the QM/MM Monte Carlo simulation. (C) Configuration of the transition state obtained from the QM/MM Monte Carlo FE simulations. Figure reproduced from ref 230. Copyright 2008 American Chemical Society.

fold efficiency.[43] Zheng et al. used the interaction energy between the TS and the enzyme to select for rate-enhancing mutations, followed by B3LYP/6-31G(d)-AMBER optimization of the reaction path to determine an activation barrier.[222] They showed that A199S/F227A/S287G/A328W/Y332G BChE had a barrier for the first step of only 10.4 kcal mol^{-1} (compared to 16.2 kcal mol^{-1} for A328W/Y332A BChE), and kinetic measurements indicated a ~2000-fold improved efficiency for cocaine hydrolysis. In vivo experiments further showed that this mutant BChE can protect mice against cocaine overdose. More recently, the full hydrolysis pathway in this efficient mutant BChE was simulated using the QM/MM-FE method.[225] This indicated that the second step, dissociation of the (−)-cocaine benzoyl ester, is rate-limiting for this mutant (ZPE-corrected barrier of 15.0 kcal mol^{-1}, versus 14.7 kcal mol^{-1} derived from experiment). Further efforts to improve catalytic activity should therefore be directed at this reaction step. Together, these calculations show how detailed knowledge of reaction mechanism from QM/MM modeling assisted in redesigning BChE into an efficient cocaine esterase.

Although efforts in improving efficiency in existing enzymes are impressive, a more ambitious goal is the *de novo* design of enzymes, especially for reactions for which no natural enzymes exists. Röthlisberger et al.[229] first used a computational design procedure based on a TS from gas phase QM calculations for Kemp elimination in 5-nitro-benzisoxazole, which was expected to be a one-step, concerted reaction. QM calculations were used to identify a set of protein groups around the TS that could maximize its stabilization, and a protein scaffold that could incorporate these groups was then selected. Catalysis in a number of the designed enzymes was investigated with QM/MM-FE calculations to calculate free energy surfaces at the PDDG/PM3-OPLS-AA level.[230] Comparison with the reaction in solution predicted the designed enzymes to be catalytic. The calculations indicated that the mechanism involved concerted proton transfer and N−O bond cleavage, although proton transfer was more advanced in the TS (Figure 6). This suggested that increasing the acidity of the catalytic base could help lower the barrier to reaction further, by stabilizing N−O bond cleavage. Subsequently, a similar protocol was used to examine catalysis by the catalytic antibody 3A4[231] and its E50D variant.[232] This suggested that the reason for the activity drop in the variant, replicated by the calculations, lies in a combination of nonoptimal substrate-base interactions, less favorable π-stacking with Trp91 in the active site, and increased contact with solvent. Kiss et al. evaluated the use of QM only calculations, ONIOM QM/MM calculations, and MM MD simulations in the computational design of Kemp eliminases.[233] They concluded that the use of extended (AMBER ff99SB) MD simulations was valuable to distinguish active from inactive designs. B3LYP/6-31+G(d,p)-AMBER calculated barriers on B3LYP/6-31G(d)-AMBER optimized conformations of the full enzyme−substrate obtained after 2 ns of MM MD yielded a reasonable correlation with experimental values, whereas QM cluster models were much less predictive. The authors concluded, however, that their ONIOM QM/MM calculations were too computationally expensive and too inaccurate to offer a useful prescreening tool in enzyme design. An EVB approach is potentially better suited for this purpose[234] due to its computationally efficient generation of free energy profiles,.[217,235] By fitting the EVB parameters to the relevant reference solution reactions calculated by *ab initio* QM methods, Frushicheva et al. obtained an impressive correlation between calculated and experimental reaction barriers for a range of enzyme−substrate combinations.[217] The results indicated that optimization of catalysis may be difficult to achieve by designed mutations in the active site, as the difference in charge distribution between the reactant and TS in the Kemp elimination reactions studied is quite small.[235] In accordance with this observation, it appeared that mutants obtained by directed evolution in this case primarily increased catalysis by reduction of solvation of the reactant state (instead of specific stabilization of the TS). Indeed, the most efficient computationally designed Kemp eliminase to date features a deeply buried active site, shielded from solvent.[236] Overall, the different examples described here indicate how QM/MM and related approaches are valuable in enzyme (re)design, by providing insight into the reaction mechanism, interactions between the active site and the reacting species as well as the effect of mutations. QM/MM methods also have the potential to improve *de novo* enzyme designs.

CONCLUSIONS AND OUTLOOK

Since the very first studies, starting 37 years ago,[6] QM/MM modeling of enzyme-catalyzed reactions has contributed to the development and testing of theories of enzyme catalysis. QM/MM methods are now regularly used to analyze of the chemistry in proteins, leading to in-depth knowledge of enzyme reaction mechanisms. When carefully applied, excellent *quantitative* agreement with experiment is also possible in certain cases.[47] It must be noted, however, that careful testing of methods (e.g., using high-level *ab initio* methods and comparison to experiment) remains important; in certain cases, 'standard' QM methods may fail to give the correct energetics.[29,30] Qualitative insight, however (e.g., prediction of relative barriers), is more easily obtained and is useful for many biochemical applications.

The examples discussed in this review demonstrate that QM/MM modeling is now increasingly used in practical applications, such as the design of drug leads and catalysts as well as understanding/predicting drug metabolism and drug resistance. These examples also show the complementarity of QM/MM modeling and experimental methods; collaboration between experimental and computational enzymologists is now common and is proving increasingly beneficial. Successful collaboration requires understanding on both sides: of the biochemical experiments, mechanistic questions, and the strengths and limitations of modeling methods. In this Current Topics article, we have focused on the use of QM/MM methods for modeling reactions, but QM/MM techniques are also increasingly being applied in other areas of biochemistry and biophysics, such as small molecule docking,[13,237] structure refinement of proteins and protein−ligand complexes,[15,238−240] and the interpretation of vibrational spectra.[16,241]

Developments in availability, flexibility, and accuracy of QM/MM methods for studying enzymes and enzyme reactions are making practical applications increasingly common. *In silico* screening of the effects of mutations on reactivity, for example, will greatly assist in the design of enzymes for specific synthetic applications and the analysis of genetic differences associated with disease or drug metabolism. Determination of enzyme reaction pathways and transition states (and, e.g., the interactions of TSs and reaction intermediates) using accurate QM/MM methods will aid efforts in structure-based drug and enzyme design, as will the combination of QM/MM calculations with more standard structure−activity relationship methods.[150,242] Overall, the impact of QM/MM modeling on enzymology and other areas of biochemistry and medicinal chemistry will certainly continue to increase.

AUTHOR INFORMATION

Corresponding Author

*Phone: +44 117 928 9097. Fax: +44 117 925 1295. E-mail: (M.W.vdK.) marc.vanderkamp@bristol.ac.uk, (A.J.M.) adrian.mulholland@bristol.ac.uk.

Funding

A.J.M. is an EPSRC Leadership Fellow, and (with M.W.vdK.) thanks the EPSRC for support (Grant Numbers EP/G007705/1 and EP/J010588/1 (CCP-BioSim)). A.J.M. also thanks NIH for support (Grant Number 1R01GM093088).

Notes

The authors declare no competing financial interest.

ABBREVIATIONS

QM/MM, quantum mechanics/molecular mechanics; MD, molecular dynamics; EVB, empirical valence bond; DFT, density functional theory; TS, transition state; TST, transition state theory; MEP, minimum energy path; PES, potential energy surface

ADDITIONAL NOTES

[a]The Web of Science database was searched with the following term: TS = ((qm/mm or mm/qm or qm-mm or mm-qm or qm:mm or mm:qm or quantum mechanics/molecular mechanics or quantum mechanical/molecular mechanical or quantum/molecular mechanic*) and (enzym*))

[b]A 'forward slash' is most commonly used in denoting QM/MM methods (though other conventions, such as QM:MM or MM/QM have been used), and we will use this form throughout the review. When explicitly stating QM and MM methods applied, however, a hyphen is used here between the QM and the MM method (because for denoting electronic structure calculations, the established nomenclature is to use a forward slash to distinguish the QM method from the basis set), e.g., B3LYP/6-31G(d)-CHARMM27. For the applications described, we have attempted to list both the QM and MM method (force field) used in this way succinctly; for full details, please refer to the original articles. It is good practice in a QM/MM application to specify clearly the MM force field (and to define any nonstandard parameters), and the QM method; this is essential for reproducibility.

REFERENCES

(1) Van der Kamp, M. W., Shaw, K. E., Woods, C. J., and Mulholland, A. J. (2008) Biomolecular simulation and modelling: status, progress and prospects. *J. R. Soc. Interface 5*, S173−S190.

(2) Masgrau, L., Roujeinikova, A., Johannissen, L. O., Hothi, P., Basran, J., Ranaghan, K. E., Mulholland, A. J., Sutcliffe, M. J., Scrutton, N. S., and Leys, D. (2006) Atomic description of an enzyme reaction dominated by proton tunneling. *Science 312*, 237−241.

(3) Hanoian, P., Sigala, P. A., Herschlag, D., and Hammes-Schiffer, S. (2010) Hydrogen Bonding in the Active Site of Ketosteroid Isomerase: Electronic Inductive Effects and Hydrogen Bond Coupling. *Biochemistry 49*, 10339−10348.

(4) Lonsdale, R., Ranaghan, K. E., and Mulholland, A. J. (2010) Computational enzymology. *Chem. Commun. 46*, 2354−2372.

(5) Senn, H. M., and Thiel, W. (2009) QM/MM Methods for Biomolecular Systems. *Angew. Chem., Int. Ed. 48*, 1198−1229.

(6) Warshel, A., and Levitt, M. (1976) Theoretical Studies of Enzymic Reactions - Dielectric, Electrostatic and Steric Stabilization of Carbonium-Ion in Reaction of Lysozyme. *J. Mol. Biol. 103*, 227−249.

(7) Kamerlin, S. C. L., and Warshel, A. (2010) At the dawn of the 21st century: Is dynamics the missing link for understanding enzyme catalysis? *Proteins: Struct., Funct. Bioinformatics 78*, 1339−1375.

(8) Warshel, A. (2003) Computer simulations of enzyme catalysis: Methods, progress, and insights. *Annu. Rev. Biophys. Biomol. Struct. 32*, 425−443.

(9) Warshel, A., Sharma, P. K., Kato, M., Xiang, Y., Liu, H. B., and Olsson, M. H. M. (2006) Electrostatic basis for enzyme catalysis. *Chem. Rev. 106*, 3210−3235.

(10) Siegbahn, P. E. M., and Himo, F. (2009) Recent developments of the quantum chemical cluster approach for modeling enzyme reactions. *J. Biol. Inorg. Chem. 14*, 643−651.

(11) Woods, C. J., Manby, F. R., and Mulholland, A. J. (2008) An efficient method for the calculation of quantum mechanics/molecular mechanics free energies. *J. Chem. Phys. 128*, No. 014109.

(12) Cho, A. E., Guallar, V., Berne, B. J., and Friesner, R. (2005) Importance of accurate charges in molecular docking: Quantum

mechanical/molecular mechanical (QM/MM) approach. *J. Comput. Chem. 26*, 915−931.
(13) Cho, A. E., Chung, J. Y., Kim, M., and Park, K. (2009) Quantum mechanical scoring for protein docking. *J. Chem. Phys. 131*, No. 134108.
(14) Ryde, U., and Nilsson, K. (2003) Quantum chemistry can locally improve protein crystal structures. *J. Am. Chem. Soc. 125*, 14232−14233.
(15) Sproviero, E., Newcomer, M., Gascón, J., Batista, E., Brudvig, G., and Batista, V. (2009) The MoD-QM/MM methodology for structural refinement of photosystem II and other biological macromolecules. *Photosynth. Res. 102*, 455−470.
(16) Barone, V., Biczysko, M., and Brancato, G. (2010) Extending the range of computational spectroscopy by QM/MM approaches: Time-dependent and time-independent routes, In *Advances in Quantum Chemistry* (John, R. S., and Erkki, B., Eds.) pp 17−57, Academic Press.
(17) Jensen, J. H., Li, H., Robertson, A. D., and Molina, P. A. (2005) Prediction and Rationalization of Protein pKa Values Using QM and QM/MM Methods. *J. Phys. Chem. A 109*, 6634−6643.
(18) Mackerell, A. D. (2004) Empirical force fields for biological macromolecules: Overview and issues. *J. Comput. Chem. 25*, 1584−1604.
(19) Ranaghan, K. E., and Mulholland, A. J. (2010) Investigations of enzyme-catalysed reactions with combined quantum mechanics/molecular mechanics (QM/MM) methods. *Int. Rev. Phys. Chem. 29*, 65−133.
(20) Senn, H. M., and Thiel, W. (2007) QM/MM methods for biological systems. *Atomistic Approaches Mod. Biol.: From Quantum Chem. Mol. Simul. 268*, 173−290.
(21) Vreven, T., Byun, K. S., Komáromi, I., Dapprich, S., Montgomery, J. A., Morokuma, K., and Frisch, M. J. (2006) Combining quantum mechanics methods with molecular mechanics methods in ONIOM. *J. Chem. Theory Comput. 2*, 815−826.
(22) Harvey, J. N. (2011) The coupled-cluster description of electronic structure: perspectives for bioinorganic chemistry. *J. Biol. Inorg. Chem. 16*, 831−839.
(23) Bowman, A. L., Ridder, L., Rietjens, I., Vervoort, J., and Mulholland, A. J. (2007) Molecular determinants of xenobiotic metabolism: QM/MM simulation of the conversion of 1-chloro-2,4-dinitrobenzene catalyzed by M1−1 glutathione *S*-transferase. *Biochemistry 46*, 6353−6363.
(24) Gao, J. L., Ma, S. H., Major, D. T., Nam, K., Pu, J. Z., and Truhlar, D. G. (2006) Mechanisms and free energies of enzymatic reactions. *Chem. Rev. 106*, 3188−3209.
(25) Nam, K., Gao, J., and York, D. M. (2008) Quantum Mechanical/Molecular Mechanical Simulation Study of the Mechanism of Hairpin Ribozyme Catalysis. *J. Am. Chem. Soc. 130*, 4680−4691.
(26) Repasky, M. P., Chandrasekhar, J., and Jorgensen, W. L. (2002) PDDG/PM3 and PDDG/MNDO: Improved semiempirical methods. *J. Comput. Chem. 23*, 1601−1622.
(27) Riccardi, D., Schaefer, P., Yang, Y., Yu, H. B., Ghosh, N., Prat-Resina, X., Konig, P., Li, G. H., Xu, D. G., Guo, H., Elstner, M., and Cui, Q. (2006) Development of effective quantum mechanical/molecular mechanical (QM/MM) methods for complex biological processes. *J. Phys. Chem. B 110*, 6458−6469.
(28) Gaus, M. G. M., Cui, Q. A., and Elstner, M. (2011) DFTB3: Extension of the Self-Consistent-Charge Density-Functional Tight-Binding Method (SCC-DFTB). *J. Chem. Theory Comput. 7*, 931−948.
(29) Van der Kamp, M. W., Żurek, J., Manby, F. R., Harvey, J. N., and Mulholland, A. J. (2010) Testing high-level QM/MM methods for modeling enzyme reactions: acetyl-CoA deprotonation in citrate synthase. *J. Phys. Chem. B 114*, 11303−11314.
(30) Lonsdale, R., Harvey, J. N., and Mulholland, A. J. (2010) Inclusion of Dispersion Effects Significantly Improves Accuracy of Calculated Reaction Barriers for Cytochrome P450 Catalyzed Reactions. *J. Phys. Chem. Lett. 1*, 3232−3237.
(31) Jurecka, P., Cerny, J., Hobza, P., and Salahub, D. R. (2007) Density functional theory augmented with an empirical dispersion term. Interaction energies and geometries of 80 noncovalent complexes compared with ab initio quantum mechanics calculations. *J. Comput. Chem. 28*, 555−569.
(32) Lonsdale, R., Harvey, J. N., and Mulholland, A. J. (2012) Effects of Dispersion in Density Functional Based Quantum Mechanical/Molecular Mechanical Calculations on Cytochrome P450 Catalyzed Reactions, *J Chem. Theory Comput. 8*, 4637−4645.
(33) Zhang, Y. (2006) Pseudobond ab initio QM/MM approach and its applications to enzyme reactions. *Theor. Chem. Acc. 116*, 43−50.
(34) Meier, K., Thiel, W., and van Gunsteren, W. F. (2012) On the effect of a variation of the force field, spatial boundary condition and size of the QM region in QM/MM MD simulations. *J. Comput. Chem. 33*, 363−378.
(35) Riccardi, D., Schaefer, P., and Cui, Q. (2005) pK_a calculations in solution and proteins with QM/MM free energy perturbation simulations: A quantitative test of QM/MM protocols. *J. Phys. Chem. B 109*, 17715−17733.
(36) Rodriguez, A., Oliva, C., Gonzalez, M., van der Kamp, M., and Mulholland, A. J. (2007) Comparison of different quantum mechanical/molecular mechanics boundary treatments in the reaction of the hepatitis C virus NS3 protease with the NS5A/5B substrate. *J. Phys. Chem. B 111*, 12909−12915.
(37) Sumowski, C. V., and Ochsenfeld, C. (2009) A Convergence Study of QM/MM Isomerization Energies with the Selected Size of the QM Region for Peptidic Systems. *J. Phys. Chem. A 113*, 11734−11741.
(38) Pezeshki, S., and Lin, H. (2011) Adaptive-Partitioning Redistributed Charge and Dipole Schemes for QM/MM Dynamics Simulations: On-the-fly Relocation of Boundaries that Pass through Covalent Bonds, *J Chem. Theory Comput. 7*, 3625−3634.
(39) Mulholland, A. J. (2005) Modelling enzyme reaction mechanisms, specificity and catalysis. *Drug Discovery Today 10*, 1393−1402.
(40) Gleeson, M. P., and Gleeson, D. (2009) QM/MM Calculations in Drug Discovery: A Useful Method for Studying Binding Phenomena? *J. Chem. Inf. Model. 49*, 670−677.
(41) Williams, I. H. (2010) Catalysis: transition-state molecular recognition? *Beilstein J. Org. Chem. 6*, 1026−1034.
(42) Martí, S., Andrés, J., Moliner, V., Silla, E., Tuñón, I., and Bertrán, J. (2008) Computational design of biological catalysts. *Chem. Soc. Rev. 37*, 2634−2643.
(43) Gao, D. Q., Cho, H., Yang, W. C., Pan, Y. M., Yang, G. F., Tai, H. H., and Zhan, C. G. (2006) Computational design of a human butyrylcholinesterase mutant for accelerating cocaine hydrolysis based on the transition-state simulation. *Angew. Chem., Int. Ed. 45*, 653−657.
(44) Claeyssens, F., Ranaghan, K. E., Lawan, N., Macrae, S. J., Manby, F. R., Harvey, J. N., and Mulholland, A. J. (2011) Analysis of chorismate mutase catalysis by QM/MM modelling of enzyme-catalysed and uncatalysed reactions. *Org. Biomol. Chem. 9*, 1578−1590.
(45) Lodola, A., Mor, M., Żurek, J., Tarzia, G., Piomelli, D., Harvey, J. N., and Mulholland, A. J. (2007) Conformational effects in enzyme catalysis: Reaction via a high energy conformation in fatty acid amide hydrolase. *Biophys. J. 92*, L20−L22.
(46) Garcia-Viloca, M., Gao, J., Karplus, M., and Truhlar, D. G. (2004) How enzymes work: analysis by modern rate theory and computer simulations. *Science 303*, 186−195.
(47) Claeyssens, F., Harvey, J. N., Manby, F. R., Mata, R. A., Mulholland, A. J., Ranaghan, K. E., Schutz, M., Thiel, S., Thiel, W., and Werner, H. J. (2006) High-accuracy computation of reaction barriers in enzymes. *Angew. Chem., Int. Ed. 45*, 6856−6859.
(48) Lonsdale, R., Hoyle, S., Grey, D. T., Ridder, L., and Mulholland, A. J. (2012) Determinants of Reactivity and Selectivity in Soluble Epoxide Hydrolase from Quantum Mechanics/Molecular Mechanics Modeling. *Biochemistry 51*, 1774−1786.
(49) Van der Kamp, M. W., McGeagh, J. D., and Mulholland, A. J. (2011) Lethal Synthesis" of fluorocitrate by citrate synthase explained through QM/MM modeling. *Angew. Chem., Int. Ed. 50*, 10349−10351.

(50) Carlson, H. A., and Jorgensen, W. L. (1996) Monte Carlo investigations of solvent effects on the chorismate to prephenate rearrangement. *J. Am. Chem. Soc. 118*, 8475.
(51) Guimaraes, C. R. W., Udier-Blagovic, M., Tubert-Brohman, I., and Jorgensen, W. L. (2005) Effects of Arg90 neutralization on the enzyme-catalyzed rearrangement of chorismate to prephenate. *J. Chem. Theory Comput. 1*, 617−625.
(52) Rosta, E., Klahn, M., and Warshel, A. (2006) Towards accurate ab initio QM/MM calculations of free-energy profiles of enzymatic reactions. *J. Phys. Chem. B 110*, 2934−2941.
(53) Hu, H., Lu, Z. Y., and Yang, W. T. (2007) QM/MM minimum free-energy path: Methodology and application to triosephosphate isomerase. *J. Chem. Theory Comput. 3*, 390−406.
(54) Thar, J., Reckien, W., and Kirchner, B. (2007) Car-Parrinello molecular dynamics simulations and biological systems, In *Atomistic Approaches in Modern Biology: From Quantum Chemistry to Molecular Simulations* (Reiher, M., Ed.) pp 133−171, Springer-Verlag, Berlin, Berlin.
(55) Hu, P., Wang, S., and Zhang, Y. (2008) Highly Dissociative and Concerted Mechanism for the Nicotinamide Cleavage Reaction in Sir2Tm Enzyme Suggested by Ab Initio QM/MM Molecular Dynamics Simulations. *J. Am. Chem. Soc. 130*, 16721−16728.
(56) Zhou, Y., Wang, S., and Zhang, Y. (2010) Catalytic Reaction Mechanism of Acetylcholinesterase Determined by Born-Oppenheimer Ab Initio QM/MM Molecular Dynamics Simulations. *J. Phys. Chem. B 114*, 8817−8825.
(57) Vocadlo, D. J., Davies, G. J., Laine, R., and Withers, S. G. (2001) Catalysis by hen egg-white lysozyme proceeds via a covalent intermediate. *Nature 412*, 835−838.
(58) Bowman, A. L., Grant, I. M., and Mulholland, A. J. (2008) QM/MM simulations predict a covalent intermediate in the hen egg white lysozyme reaction with its natural substrate. *Chem. Commun.*, 4425−4427.
(59) Phillips, D. C. (1967) Hen Egg-White Lysozyme Molecule. *Proc. Natl. Acad. Sci. U. S. A. 57*, 484.
(60) Kirby, A. J. (2001) The lysozyme mechanism sorted - after 50 years. *Nat. Struct. Biol. 8*, 737−739.
(61) Koshland, D. E. (1953) Stereochemistry and the Mechanism of Enzymatic Reactions. *Biol. Rev. Camb. Philos. Soc. 28*, 416−436.
(62) Biarnes, X., Ardevol, A., Iglesias-Fernandez, J., Planas, A., and Rovira, C. (2011) Catalytic Itinerary in 1,3−1,4-beta-Glucanase Unraveled by QM/MM Metadynamics. Charge Is Not Yet Fully Developed at the Oxocarbenium Ion-like Transition State. *J. Am. Chem. Soc. 133*, 20301−20309.
(63) Gomez, H., Polyak, I., Thiel, W., Lluch, J. M., and Masgrau, L. (2012) Retaining Glycosyltransferase Mechanism Studied by QM/MM Methods: Lipopolysaccharyl-alpha-1,4-galactosyltransferase C Transfers alpha-Galactose via an Oxocarbenium Ion-like Transition State. *J. Am. Chem. Soc. 134*, 4743−4752.
(64) Pierdominici-Sottile, G., Horenstein, N. A., and Roitberg, A. E. (2011) Free Energy Study of the Catalytic Mechanism of Trypanosoma cruzitrans-Sialidase. From the Michaelis Complex to the Covalent Intermediate. *Biochemistry 50*, 10150−10158.
(65) Mulholland, A. J., and Richards, W. G. (1997) Acetyl-CoA enolization in citrate synthase: a quantum mechanical/molecular mechanical (QM/MM) study. *Proteins: Struct., Funct. Genet. 27*, 9−25.
(66) Mulholland, A. J., Lyne, P. D., and Karplus, M. (2000) Ab initio QM/MM study of the citrate synthase mechanism. A low-barrier hydrogen bond is not involved. *J. Am. Chem. Soc. 122*, 534−535.
(67) Van der Kamp, M. W., Perruccio, F., and Mulholland, A. J. (2007) Ab initio QM/MM modelling of acetyl-CoA deprotonation in the enzyme citrate synthase. *J. Mol. Graph. Model. 26*, 596−601.
(68) Kurz, L. C., Ackerman, J. J. H., and Drysdale, G. R. (1985) Evidence from C-13 NMR for polarization of the carbonyl of oxaloacetate in the active-site of citrate synthase. *Biochemistry 24*, 452−457.
(69) Van der Kamp, M. W., Perruccio, F., and Mulholland, A. J. (2007) Substrate polarization in enzyme catalysis: QM/MM analysis of the effect of oxaloacetate polarization on acetyl-CoA enolization in citrate synthase. *Proteins: Struct., Funct. Bioinformatics 69*, 521−535.
(70) Grimme, S. (2003) Improved second-order Møller−Plesset perturbation theory by separate scaling of parallel- and antiparallel-spin pair correlation energies. *J. Chem. Phys. 118*, 9095−9102.
(71) Eggerer, H. (1965) Zum Mechanismus der biologischen Umwandlung von Citronensaure. VI. Citrat-Synthase ist eine Acetyl-CoA Enolase. *Biochem. Z. 343*, 111−138.
(72) Kurz, L. C., Constantine, C. Z., Jiang, H., and Kappock, T. J. (2009) The partial substrate dethiaacetyl-coenzyme a mimics all critical carbon acid reactions in the condensation half-reaction catalyzed by *Thermoplasma acidophilum* citrate synthase. *Biochemistry 48*, 7878−7891.
(73) Karpusas, M., Branchaud, B., and Remington, S. J. (1990) Proposed mechanism for the condensation reaction of citrate synthase: 1.9 Å structure of the ternary complex with oxaloacetate and carboxymethyl coenzyme-A. *Biochemistry 29*, 2213−2219.
(74) Remington, S. J. (1992) Structure and mechanism of citrate synthase. *Curr. Top. Cell. Regul. 33*, 209−229.
(75) Mulholland, A. J., and Richards, W. G. (1998) A model of the condensation step in the citrate synthase reaction. *Theochem-J. Mol. Struct. 427*, 175−184.
(76) Van der Kamp, M. W., Perruccio, F., and Mulholland, A. J. (2008) High-level QM/MM modelling predicts an arginine as the acid in the condensation reaction catalysed by citrate synthase. *Chem. Commun.*, 1874−1876.
(77) Alter, G. M., Casazza, J. P., Wang, Z., Nemeth, P., Srere, P. A., and Evans, C. T. (1990) Mutation of essential catalytic residues in pig citrate synthase. *Biochemistry 29*, 7557−7563.
(78) Cleland, W. W., and Kreevoy, M. M. (1994) Low-barrier hydrogen-bonds and enzymatic catalysis. *Science 264*, 1887−1890.
(79) Hur, S., and Bruice, T. C. (2003) Comparison of formation of reactive conformers (NACs) for the Claisen rearrangement of chorismate to prephenate in water and in the E-coli mutase: The efficiency of the enzyme catalysi. *J. Am. Chem. Soc. 125*, 5964−5972.
(80) Eisenmesser, E. Z., Millet, O., Labeikovsky, W., Korzhnev, D. M., Wolf-Watz, M., Bosco, D. A., Skalicky, J. J., Kay, L. E., and Kern, D. (2005) Intrinsic dynamics of an enzyme underlies catalysis. *Nature 438*, 117−121.
(81) Kohen, A., and Klinman, J. P. (1998) Enzyme catalysis: Beyond classical paradigms. *Acc. Chem. Res. 31*, 397−404.
(82) Kamerlin, S. C. L., Mavri, J., and Warshel, A. (2010) Examining the case for the effect of barrier compression on tunneling, vibrationally enhanced catalysis, catalytic entropy and related issues. *FEBS Lett. 584*, 2759−2766.
(83) Kamerlin, S. C. L., and Warshel, A. (2010) An analysis of all the relevant facts and arguments indicates that enzyme catalysis does not involve large contributions from nuclear tunneling. *J. Phys. Org. Chem. 23*, 677−684.
(84) Olsson, M. H. M., Parson, W. W., and Warshel, A. (2006) Dynamical contributions to enzyme catalysis: Critical tests of a popular hypothesis. *Chem. Rev. 106*, 1737−1756.
(85) Kanaan, N., Ferrer, S., Martí, S., Garcia-Viloca, M., Kohen, A., and Moliner, V. (2011) Temperature Dependence of the Kinetic Isotope Effects in Thymidylate Synthase. A Theoretical Study. *J. Am. Chem. Soc. 133*, 6692−6702.
(86) Liu, Y. P., Lynch, G. C., Truong, T. N., Lu, D. H., Truhlar, D. G., and Garrett, B. C. (1993) Molecular modeling of the kinetic isotope effect for the [1,5] sigmatropic rearrangement of cis-1,3-pentadiene. *J. Am. Chem. Soc. 115*, 2408−2415.
(87) Masgrau, L., Ranaghan, K. E., Scrutton, N. S., Sutcliffe, M. J., and Mulholland, A. J. (2007) Tunneling and classical paths for proton transfer in an enzyme reaction dominated by tunneling: Oxidation of tryptamine by aromatic amine dehydrogenase. *J. Phys. Chem. B 111*, 3032−3047.
(88) Ranaghan, K. E., Masgrau, L., Scrutton, N. S., Sutcliffe, M. J., and Mulholland, A. J. (2007) Analysis of classical and quantum paths for deprotonation of methylamine by methylamine dehydrogenase. *ChemPhysChem 8*, 1816−1835.

(89) Schwartz, S. D., and Schramm, V. L. (2009) Enzymatic transition states and dynamic motion in barrier crossing. *Nat. Chem. Biol. 5*, 552−559.
(90) Canepa, C. (2010) A stationary-wave model of enzyme catalysis. *J. Comput. Chem. 31*, 343−350.
(91) Mata, R. A., Werner, H. J., Thiel, S., and Thiel, W. (2008) Toward accurate barriers for enzymatic reactions: QM/MM case study on p-hydroxybenzoate hydroxylase. *J. Chem. Phys. 128*, No. 025104.
(92) Lonsdale, R., Harvey, J. N., Manby, F. R., and Mulholland, A. J. (2011) Comment on "A Stationary-Wave Model of Enzyme Catalysis" By Carlo Canepa. *J. Comput. Chem. 32*, 368−369.
(93) Olsson, M. H. M., Mavri, J., and Warshel, A. (2006) Transition state theory can be used in studies of enzyme catalysis: lessons from simulations of tunnelling and dynamical effects in lipoxygenase and other systems. *Phil. Trans. R. Soc. B 361*, 1417−1432.
(94) McGeagh, J. D., Ranaghan, K. E., and Mulholland, A. J. (2011) Protein dynamics and enzyme catalysis: Insights from simulations. *Biochim. Biophys. Acta-Proteins Proteomics 1814*, 1077−1092.
(95) Ridder, L., Mulholland, A. J., Rietjens, I., and Vervoort, J. (2000) A quantum mechanical/molecular mechanical study of the hydroxylation of phenol and halogenated derivatives by phenol hydroxylase. *J. Am. Chem. Soc. 122*, 8728−8738.
(96) Ridder, L., Mulholland, A. J., Vervoort, J., and Rietjens, I. (1998) Correlation of calculated activation energies with experimental rate constants for an enzyme catalyzed aromatic hydroxylation. *J. Am. Chem. Soc. 120*, 7641−7642.
(97) Friesner, R. A., and Guallar, V. (2005) Ab initio quantum chemical and mixed quantum mechanics/molecular mechanics (QM/MM) methods for studying enzymatic catalysis. *Annu. Rev. Phys. Chem. 56*, 389−427.
(98) Pisliakov, A. V., Cao, J., Kamerlin, S. C. L., and Warshel, A. (2009) Enzyme millisecond conformational dynamics do not catalyze the chemical step. *Proc. Natl. Acad. Sci. U. S. A. 106*, 17359−17364.
(99) Nashine, V. C., Hammes-Schiffer, S., and Benkovic, S. J. (2010) Coupled motions in enzyme catalysis. *Curr. Opin. Chem. Biol. 14*, 644−651.
(100) Ma, B., and Nussinov, R. (2010) Enzyme dynamics point to stepwise conformational selection in catalysis. *Curr. Opin. Chem. Biol. 14*, 652−659.
(101) Castillo, R., Roca, M., Soriano, A., Moliner, V., and Tuñón, I. (2008) Using Grote-Hynes theory to quantify dynamical effects on the reaction rate of enzymatic processes. The case of methyltransferases. *J. Phys. Chem. B 112*, 529−534.
(102) Kanaan, N., Roca, M., Tuñón, I., Martí, S., and Moliner, V. (2010) Theoretical study of the temperature dependence of dynamic effects in thymidylate synthase. *Phys. Chem. Chem. Phys. 12*, 11657−11664.
(103) Roca, M., Oliva, M., Castillo, R., Moliner, V., and Tuñón, I. (2010) Do dynamic effects play a significant role in enzymatic catalysis? A theoretical analysis of formate dehydrogenase. *Chem.—Eur. J. 16*, 11399−11411.
(104) Ruiz-Pernia, J. J., Tuñón, I., Moliner, V., Hynes, J. T., and Roca, M. (2008) Dynamic effects on reaction rates in a Michael addition catalyzed by chalcone isomerase. Beyond the frozen environment approach. *J. Am. Chem. Soc. 130*, 7477−7488.
(105) Kamerlin, S. C. L., and Warshel, A. (2010) Reply to Karplus: Conformational dynamics have no role in the chemical step. *Proc. Natl. Acad. Sci. U. S. A. 107*, E72−E72.
(106) Strajbl, M., Shurki, A., Kato, M., and Warshel, A. (2003) Apparent NAC effect in chorismate mutase reflects electrostatic transition state stabilization. *J. Am. Chem. Soc. 125*, 10228−10237.
(107) Ranaghan, K. E., and Mulholland, A. J. (2004) Conformational effects in enzyme catalysis: QM/MM free energy calculation of the 'NAC' contribution in chorismate mutase. *Chem. Commun.*, 1238−1239.
(108) Martí, S., Roca, M., Andrés, J., Moliner, V., Silla, E., Tuñón, I., and Bertrán, J. (2004) Theoretical insights in enzyme catalysis. *Chem. Soc. Rev. 33*, 98−107.
(109) Lyne, P. D., Mulholland, A. J., and Richards, W. G. (1995) Insights into Chorismate Mutase Catalysis from a Combined QM/MM Simulation of the Enzyme Reaction. *J. Am. Chem. Soc. 117*, 11345−11350.
(110) Ranaghan, K. E., Ridder, L., Szefczyk, B., Sokalski, W. A., Hermann, J. C., and Mulholland, A. J. (2003) Insights into enzyme catalysis from QM/MM modelling: transition state stabilisation in chorismate mutase. *Mol. Phys. 101*, 2695−2714.
(111) Martí, S., Andrés, J., Moliner, V., Silla, E., Tuñón, I., and Bertrán, J. (2003) Preorganisation and reorganisation as related factors in enzyme catalysis: The chorismate mutase case. *Chem.—Eur. J. 9*, 984−991.
(112) Claeyssens, F., Ranaghan, K., Manby, F., Harvey, J., and Mulholland, A. (2005) Multiple high-level QM/MM reaction paths demonstrate transition-state stabilization in chorismate mutase: correlation of barrier height with transition-state stabilization. *Chem. Commun.*, 5068−5070.
(113) Ishida, T. (2010) Effects of Point Mutation on Enzymatic Activity: Correlation between Protein Electronic Structure and Motion in Chorismate Mutase Reaction. *J. Am. Chem. Soc. 132*, 7104−7118.
(114) Szefczyk, B., Mulholland, A. J., Ranaghan, K. E., and Sokalski, W. A. (2004) Differential transition-state stabilization in enzyme catalysis: Quantum chemical analysis of interactions in the chorismate mutase reaction and prediction of the optimal catalytic field. *J. Am. Chem. Soc. 126*, 16148−16159.
(115) Allemann, R. K., and Scrutton, N. S., Eds. (2009) *Quantum Tunnelling in Enzyme-catalysed Reactions*, RSC, Cambridge, UK.
(116) Grant, K. L., and Klinman, J. P. (1989) Evidence that protium and deuterium undergo significant tunneling in the reaction catalyzed by bovine serum amine oxidase. *Biochemistry 28*, 6597−6605.
(117) Cha, Y., Murray, C. J., and Klinman, J. P. (1989) Hydrogen tunneling in enzyme reactions. *Science 243*, 1325−1330.
(118) Glickman, M. H., and Klinman, J. P. (1995) Nature of Rate-Limiting Steps in the Soybean Lipoxygenase-1 Reaction. *Biochemistry 34*, 14077−14092.
(119) Hay, S., and Scrutton, N. S. (2012) Good vibrations in enzyme-catalysed reactions. *Nat. Chem. 4*, 161−168.
(120) Hay, S., Sutcliffe, M. J., and Scrutton, N. S. (2007) Promoting motions in enzyme catalysis probed by pressure studies of kinetic isotope effects. *Proc. Natl. Acad. Sci. U. S. A. 104*, 507−512.
(121) Liu, H. B., and Warshel, A. (2007) Origin of the temperature dependence of isotope effects in enzymatic reactions: The case of dihydrofolate reductase. *J. Phys. Chem. B 111*, 7852−7861.
(122) Williams, I. H. (2010) Quantum catalysis? A comment on tunnelling contributions for catalysed and uncatalysed reactions. *J. Phys. Org. Chem. 23*, 685−689.
(123) Glowacki, D. R., Harvey, J. N., and Mulholland, A. J. (2012) Taking Ockham's razor to enzyme dynamics and catalysi. *Nat. Chem. 4*, 169−176.
(124) Roston, D., Cheatum, C. M., and Kohen, A. (2012) Hydrogen donor−acceptor fluctuations from kinetic isotope effects: A phenomenological model. *Biochemistry 51*, 6860−6870.
(125) Agrawal, N., Lesley, S. A., Kuhn, P., and Kohen, A. (2004) Mechanistic studies of a flavin-dependent thymidylate synthase. *Biochemistry 43*, 10295−10301.
(126) Kanaan, N., Martí, S., Moliner, V., and Kohen, A. (2007) A quantum mechanics/molecular mechanics study of the catalytic mechanism of the thymidylate synthase. *Biochemistry 46*, 3704−3713.
(127) Kanaan, N., Martí, S., Moliner, V., and Kohen, A. (2009) QM/MM Study of Thymidylate Synthase: Enzymatic Motions and the Temperature Dependence of the Rate Limiting Step. *J. Phys. Chem. A 113*, 2176−2182.
(128) Garcia-Viloca, M., Alhambra, C., Truhlar, D. G., and Gao, J. (2001) Inclusion of quantum-mechanical vibrational energy in reactive potentials of mean force. *J. Chem. Phys. 114*, 9953−9958.
(129) Gertner, B. J., Wilson, K. R., and Hynes, J. T. (1989) Nonequilibrium solvation effects on reaction-rates for model S_N2 reactions in water. *J. Chem. Phys. 90*, 3537−3558.

(130) Grote, R. F., and Hynes, J. T. (1980) The stable states picture of chemical-reactions. 2. Rate constants for condensed and gas-phase reaction models. *J. Chem. Phys. 73*, 2715−2732.
(131) Lu, D. H., Truong, T. N., Melissas, V. S., Lynch, G. C., Liu, Y. P., Garrett, B. C., Steckler, R., Isaacson, A. D., Rai, S. N., Hancock, G. C., Lauderdale, J. G., Joseph, T., and Truhlar, D. G. (1992) POLYRATE4: a New Version of a Computer-Program for the Calculation of Chemical-Reaction Rates for Polyatomics. *Comput. Phys. Commun. 71*, 235−262.
(132) Zhang, Y., Kua, J., and McCammon, J. A. (2002) Role of the Catalytic Triad and Oxyanion Hole in Acetylcholinesterase Catalysis: An ab initio QM/MM Study. *J. Am. Chem. Soc. 124*, 10572−10577.
(133) Fuxreiter, M., and Warshel, A. (1998) Origin of the catalytic power of acetylcholinesterase: Computer simulation studies. *J. Am. Chem. Soc. 120*, 183−194.
(134) Topf, M., Várnai, P., and Richards, W. G. (2002) Ab Initio QM/MM Dynamics Simulation of the Tetrahedral Intermediate of Serine Proteases: Insights into the Active Site Hydrogen-Bonding Network. *J. Am. Chem. Soc. 124*, 14780−14788.
(135) Ishida, T. (2006) Low-Barrier Hydrogen Bond Hypothesis in the Catalytic Triad Residue of Serine Proteases: Correlation between Structural Rearrangement and Chemical Shifts in the Acylation Process†. *Biochemistry 45*, 5413−5420.
(136) Schutz, C. N., and Warshel, A. (2004) The low barrier hydrogen bond (LBHB) proposal revisited: The case of the asp... his pair in serine proteases. *Proteins: Struct., Funct. Bioinformatics 55*, 711−723.
(137) Vagedes, P., Rabenstein, B., Aqvist, J., Marelius, J., and Knapp, E. W. (2000) The deacylation step of acetylcholinesterase: Computer simulation studies. *J. Am. Chem. Soc. 122*, 12254−12262.
(138) Froede, H. C., and Wilson, I. B. (1984) Direct determination of acetyl-enzyme intermediate in the acetylcholinesterase-catalyzed hydrolysis of acetylcholine and acetylthiocholine. *J. Biol. Chem. 259*, 1010−1013.
(139) Nemukhin, A. V., Lushchekina, S. V., Bochenkova, A. V., Golubeva, A. A., and Varfolomeev, S. D. (2008) Characterization of a complete cycle of acetylcholinesterase catalysis by ab initio QM/MM modeling. *J. Mol. Model. 14*, 409−416.
(140) Chen, X., Fang, L., Liu, J., and Zhan, C.-G. (2011) Reaction pathway and free energy profile for butyrylcholinesterase-catalyzed hydrolysis of acetylcholine. *J. Phys. Chem. B 115*, 1315−1322.
(141) Boeck, A. T., Schopfer, L. M., and Lockridge, O. (2002) DNA sequence of butyrylcholinesterase from the rat: expression of the protein and characterization of the properties of rat butyrylcholinesterase. *Biochem. Pharmacol. 63*, 2101−2110.
(142) Chen, X., Fang, L., Liu, J. J., and Zhan, C. G. (2012) Reaction Pathway and Free Energy Profiles for Butyrylcholinesterase-Catalyzed Hydrolysis of Acetylthiocholine. *Biochemistry 51*, 1297−1305.
(143) Bourne, Y., Kolb, H. C., Radić, Z., Sharpless, K. B., Taylor, P., and Marchot, P. (2004) Freeze-frame inhibitor captures acetylcholinesterase in a unique conformation. *Proc. Natl. Acad. Sci. U. S. A. 101*, 1449−1454.
(144) Senapati, S., Cheng, Y., and McCammon, J. A. (2006) In-situ synthesis of a tacrine-triazole-based Inhibitor of acetylcholinesterase: Configurational selection imposed by steric interactions. *J. Med. Chem. 49*, 6222−6230.
(145) Cheng, Y. H., Cheng, X. L., Radic, Z., and McCammon, J. A. (2007) Acetylcholinesterase: Mechanisms of covalent inhibition of wild-type and H447I mutant determined by computational analyses. *J. Am. Chem. Soc. 129*, 6562−6570.
(146) Liu, J., Zhang, Y., and Zhan, C.-G. (2009) Reaction Pathway and Free-Energy Barrier for Reactivation of Dimethylphosphoryl-Inhibited Human Acetylcholinesterase. *J. Phys. Chem. B 113*, 16226−16236.
(147) Kwasnieski, O., Verdier, L., Malacria, M., and Derat, E. (2009) Fixation of the Two Tabun Isomers in Acetylcholinesterase: A QM/MM Study. *J. Phys. Chem. B 113*, 10001−10007.
(148) Beck, J. M., and Hadad, C. M. (2010) Reaction profiles of the interaction between sarin and acetylcholinesterase and the S203C mutant: Model nucleophiles and QM/MM potential energy surfaces. *Chem. Biol. Interact. 187*, 220−224.
(149) Minkkila, A., Saario, S. M., and Nevalainen, T. (2010) Discovery and Development of Endocannabinoid-Hydrolyzing Enzyme Inhibitors. *Curr. Top. Med. Chem. 10*, 828−858.
(150) Lodola, A., Mor, M., Hermann, J. C., Tarzia, G., Piomelli, D., and Mulholland, A. J. (2005) QM/MM modelling of oleamide hydrolysis in fatty acid amide hydrolase (FAAH) reveals a new mechanism of nucleophile activation. *Chem. Commun.*, 4399−4401.
(151) Tubert-Brohman, I., Acevedo, O., and Jorgensen, W. L. (2006) Elucidation of hydrolysis mechanisms for fatty acid amide hydrolase and its Lys142Ala variant via QM/MM simulations. *J. Am. Chem. Soc. 128*, 16904−16913.
(152) Lodola, A., Sirirak, J., Fey, N., Rivara, S., Mor, M., and Mulholland, A. J. (2010) Structural Fluctuations in Enzyme-Catalyzed Reactions: Determinants of Reactivity in Fatty Acid Amide Hydrolase from Multivariate Statistical Analysis of Quantum Mechanics/Molecular Mechanics Paths. *J. Chem. Theory Comput. 6*, 2948−2960.
(153) Lodola, A., Mor, M., Rivara, S., Christov, C., Tarzia, G., Piomelli, D., and Mulholland, A. J. (2008) Identification of productive inhibitor binding orientation in fatty acid amide hydrolase (FAAH) by QM/MM mechanistic modelling. *Chem. Commun.*, 214−216.
(154) Lodola, A., Rivara, S., and Mor, M. (2011) Application of Computational Methods to the Design of Fatty Acid Amide Hydrolase (FAAH) Inhibitors Based on a Carbamic Template Structure, In *Advances in Protein Chemistry and Structural Biology* (Christov. C. Ed.) pp 1−26, Academic Press, New York.
(155) Mor, M., Lodola, A., Rivara, S., Vacondio, F., Duranti, A., Tontini, A., Sanchini, S., Piersanti, G., Clapper, J. R., King, A. R., Tarzia, G., and Piomelli, D. (2008) Synthesis and Quantitative Structure−Activity Relationship of Fatty Acid Amide Hydrolase Inhibitors: Modulation at the N-Portion of Biphenyl-3-yl Alkylcarbamates. *J. Med. Chem. 51*, 3487−3498.
(156) Mileni, M., Kamtekar, S., Wood, D. C., Benson, T. E., Cravatt, B. F., and Stevens, R. C. (2010) Crystal Structure of Fatty Acid Amide Hydrolase Bound to the Carbamate Inhibitor URB597: Discovery of a Deacylating Water Molecule and Insight into Enzyme Inactivation. *J. Mol. Biol. 400*, 743−754.
(157) Lodola, A., Capoferri, L., Rivara, S., Chudyk, E., Sirirak, J., Dyguda-Kazimierowicz, E., Sokalski, W. A., Mileni, M., Tarzia, G., Piomelli, D., Mor, M., and Mulholland, A. J. (2011) Understanding the role of carbamate reactivity in fatty acid amide hydrolase inhibition by QM/MM mechanistic modelling. *Chem. Commun. 47*, 2517−2519.
(158) Piana, S., Bucher, D., Carloni, P., and Röthlisberger, U. (2004) Reaction mechanism of HIV-1 protease by hybrid carparrinello/classical MD simulations. *J. Phys. Chem. B 108*, 11139−11149.
(159) Rungrotmongkol, T., Hannongbua, S., and Mulholland, A. (2004) Mechanistic study of HIV-1 reverse transcriptase at the active site based on QM/MM method. *J. Theor. Comput. Chem. 3*, 491−500.
(160) Rungrotmongkol, T., Mulholland, A. J., and Hannongbua, S. (2007) Active site dynamics and combined quantum mechanics/molecular mechanics (QM/MM) modelling of a HIV-1 reverse transcriptase/DNA/dTTP complex. *J. Mol. Graph. Model. 26*, 1−13.
(161) Carnevale, V., Raugei, S., Piana, S., and Carloni, P. (2008) On the nature of the reaction intermediate in the HIV-1 protease: a quantum chemical study. *Comput. Phys. Commun. 179*, 120−123.
(162) Ruiz-Pernia, J. J., Alves, C. N., Moliner, V., Silla, E., and Tuñón, I. (2009) A QM/MM study of the reaction mechanism for the 3'-processing step catalyzed by HIV-1 integrase. *J. Mol. Struct.-Theochem 898*, 115−120.
(163) Trylska, J., Grochowski, P., and McCammon, J. A. (2004) The role of hydrogen bonding in the enzymatic reaction catalyzed by HIV-1 protease. *Protein Sci. 13*, 513−528.
(164) Das, A., Mahale, S., Prashar, V., Bihani, S., Ferrer, J. L., and Hosur, M. V. (2010) X-ray snapshot of HIV-1 protease in action: observation of tetrahedral intermediate and short ionic hydrogen bond SIHB with catalytic aspartate. *J. Am. Chem. Soc. 132*, 6366−6373.

(165) Garrec, J., Sautet, P., and Fleurat-Lessard, P. (2011) Understanding the HIV-1 Protease Reactivity with DFT: What Do We Gain from Recent Functionals? *J. Phys. Chem. B 115*, 8545−8558.
(166) Suresh, C. H., Vargheese, A. M., Vijayalakshmi, K. P., Mohan, N., and Koga, N. (2008) Role of structural water molecule in HIV protease-inhibitor complexes: A QM/MM study. *J. Comput. Chem. 29*, 1840−1849.
(167) Hensen, C., Hermann, J. C., Nam, K. H., Ma, S. H., Gao, J. L., and Höltje, H. D. (2004) A combined QM/MM approach to protein-ligand interactions: Polarization effects of the HIV-1 protease on selected high affinity inhibitors. *J. Med. Chem. 47*, 6673−6680.
(168) Garrec, J., Cascella, M., Röthlisberger, U., and Fleurat-Lessard, P. (2010) Low inhibiting power of N···CO based peptidomimetic compounds against HIV-1 protease: Insights from a QM/MM study. *J. Chem. Theory Comput. 6*, 1369−1379.
(169) Gautier, A., Pitrat, D., and Hasserodt, J. (2006) An unusual functional group interaction and its potential to reproduce steric and electrostatic features of the transition states of peptidolysis. *Biorg. Med. Chem. 14*, 3835−3847.
(170) Makatini, M. M., Petzold, K., Sriharsha, S. N., Ndlovu, N., Soliman, M. E. S., Honarparvar, B., Parboosing, R., Naidoo, A., Arvidsson, P. I., Sayed, Y., Govender, P., Maguire, G. E. M., Kruger, H. G., and Govender, T. (2011) Synthesis and structural studies of pentacycloundecane-based HIV-1 PR inhibitors: A hybrid 2D NMR and docking/QM/MM/MD approach. *Eur. J. Med. Chem. 46*, 3976−3985.
(171) Shaik, S., Cohen, S., Wang, Y., Chen, H., Kumar, D., and Thiel, W. (2010) P450 Enzymes: Their Structure, Reactivity, and Selectivity-Modeled by QM/MM Calculations. *Chem. Rev. 110*, 949−1017.
(172) Lonsdale, R., Harvey, J. N., and Mulholland, A. J. (2012) A practical guide to modelling enzyme-catalysed reactions. *Chem. Soc. Rev. 41*, 3025−3038.
(173) Porro, C. S., Sutcliffe, M. J., and de Visser, S. P. (2009) Quantum Mechanics/Molecular Mechanics Studies on the Sulfoxidation of Dimethyl Sulfide by Compound I and Compound 0 of Cytochrome P450: Which Is the Better Oxidant?†. *J. Phys. Chem. A 113*, 11635−11642.
(174) Lai, W. Z., and Shaik, S. (2011) Can Ferric-Superoxide Act as a Potential Oxidant in P450(cam)? QM/MM Investigation of Hydroxylation, Epoxidation, and Sulfoxidation. *J. Am. Chem. Soc. 133*, 5444−5452.
(175) Bathelt, C. M., Żurek, J., Mulholland, A. J., and Harvey, J. N. (2005) Electronic structure of compound I in human isoforms of cytochrome P450 from QM/MM modeling. *J. Am. Chem. Soc. 127*, 12900−12908.
(176) Fishelovitch, D., Hazan, C., Hirao, H., Wolfson, H. J., Nussinov, R., and Shaik, S. (2007) QM/MM study of the active species of the human cytochrome p450 3A4, and the influence thereof of the multiple substrate binding. *J. Phys. Chem. B 111*, 13822−13832.
(177) Shou, M. G., Mei, Q., Ettore, M. W., Dai, R. K., Baillie, T. A., and Rushmore, T. H. (1999) Sigmoidal kinetic model for two co-operative substrate-binding sites in a cytochrome P450 3A4 active site: an example of the metabolism of diazepam and its derivatives. *Biochem. J. 340*, 845−853.
(178) Harvey, J. N., Bathelt, C. M., and Mulholland, A. J. (2006) QM/MM modeling of compound I active species in cytochrome P450, Cytochrome c Peroxidase, and Ascorbate Peroxidase. *J. Comput. Chem. 27*, 1352−1362.
(179) Lonsdale, R., Oláh, J., Mulholland, A. J., and Harvey, J. N. (2011) Does Compound I vary significantly between isoforms of Cytochrome P450? *J. Am. Chem. Soc. 133*, 15464−15474.
(180) Lonsdale, R., Harvey, J. N., and Mulholland, A. J. (2010) Compound I Reactivity Defines Alkene Oxidation Selectivity in Cytochrome P450cam. *J. Phys. Chem. B 114*, 1156−1162.
(181) Altun, A., Guallar, V., Friesner, R. A., Shaik, S., and Thiel, W. (2006) The effect of heme environment on the hydrogen abstraction reaction of camphor in P450(cam) catalysis: A QM/MM study. *J. Am. Chem. Soc. 128*, 3924−3925.
(182) Altun, A., Shaik, S., and Thiel, W. (2006) Systematic QM/MM investigation of factors that affect the cytochrome P450-catalyzed hydrogen abstraction of camphor. *J. Comput. Chem. 27*, 1324−1337.
(183) Cohen, S., Kozuch, S., Hazan, C., and Shaik, S. (2006) Does substrate oxidation determine the regioselectivity of cyclohexene and propene oxidation by cytochrome P450? *J. Am. Chem. Soc. 128*, 11028−11029.
(184) Schoneboom, J. C., Cohen, S., Lin, H., Shaik, S., and Thiel, W. (2004) Quantum mechanical/molecular mechanical investigation of the mechanism of C-H hydroxylation of camphor by cytochrome P450(cam): Theory supports a two-state rebound mechanism. *J. Am. Chem. Soc. 126*, 4017−4034.
(185) Żurek, J., Foloppe, N., Harvey, J. N., and Mulholland, A. J. (2006) Mechanisms of reaction in cytochrome P450: hydroxylation of camphor in P450cam. *Org. Biomol. Chem. 4*, 3931−3937.
(186) Oláh, J., Mulholland, A. J, and Harvey, J. N. (2011) Understanding the determinants of selectivity in drug metabolism through modeling of dextromethorphan oxidation by cytochrome P450. *Proc. Natl. Acad. Sci. U. S. A. 108*, 6050−6055.
(187) Li, D. M., Huang, X. Q., Han, K. L., and Zhan, C. G. (2011) Catalytic Mechanism of Cytochrome P450 for 5 '-Hydroxylation of Nicotine: Fundamental Reaction Pathways and Stereoselectivity. *J. Am. Chem. Soc. 133*, 7416−7427.
(188) Lai, W., Chen, H., Cohen, S., and Shaik, S. (2011) Will P450(cam) Hydroxylate or Desaturate Alkanes? QM and QM/MM Studies. *J. Phys. Chem. Lett. 2*, 2229−2235.
(189) Usharani, D., Zazza, C., Lai, W. Z., Chourasia, M., Waskell, L., and Shaik, S. (2012) A Single-Site Mutation (F429H) Converts the Enzyme CYP 2B4 into a Heme Oxygenase: A QM/MM Study. *J. Am. Chem. Soc. 134*, 4053−4056.
(190) Roca, M., Martí, S., Andrés, J., Moliner, V., Tuñón, I., Bertrán, J., and Williams, I. H. (2003) Theoretical Modeling of Enzyme Catalytic Power: Analysis of "Cratic" and Electrostatic Factors in Catechol O-Methyltransferase. *J. Am. Chem. Soc. 125*, 7726−7737.
(191) Lin, P., Yang, W., Pedersen, L. C., Negishi, M., and Pedersen, L. G. (2006) Searching for the minimum energy path in the sulfuryl transfer reaction catalyzed by human estrogen sulfotransferase: Role of enzyme dynamics. *Int. J. Quantum Chem. 106*, 2981−2998.
(192) Dourado, D., Fernandes, P. A., Mannervik, B., and Ramos, M. J. (2008) Glutathione transferase: New model for glutathione activation. *Chem.—Eur. J. 14*, 9591−9598.
(193) Ridder, L., Rietjens, I., Vervoort, J., and Mulholland, A. J. (2002) Quantum mechanical/molecular mechanical free energy simulations of the glutathione S-transferase (M1−1) reaction with phenanthrene 9,10-oxide. *J. Am. Chem. Soc. 124*, 9926−9936.
(194) Calvaresi, M., Stenta, M., Garavelli, M., Altoe, P., and Bottoni, A. (2012) Computational Evidence for the Catalytic Mechanism of Human Glutathione S-Transferase A3−3: A QM/MM Investigation. *ACS Catal. 2*, 280−286.
(195) Parker, L. J., Italiano, L. C., Morton, C. J., Hancock, N. C., Ascher, D. B., Aitken, J. B., Harris, H. H., Campomanes, P., Röthlisberger, U., De Luca, A., Lo Bello, M., Ang, W. H., Dyson, P. J., and Parker, M. W. (2011) Studies of Glutathione Transferase P1−1 Bound to a Platinum(IV)-Based Anticancer Compound Reveal the Molecular Basis of Its Activation. *Chem.—Eur. J. 17*, 7806−7816.
(196) Hermann, J. C., Ridder, L., Mulholland, A. J., and Höltje, H. D. (2003) Identification of Glu166 as the general base in the acylation reaction of class A beta-lactamases through QM/MM modeling. *J. Am. Chem. Soc. 125*, 9590−9591.
(197) Hermann, J. C., Hensen, C., Ridder, L., Mulholland, A. J., and Höltje, H. D. (2005) Mechanisms of antibiotic resistance: QM/MM modeling of the acylation reaction of a class A beta-lactamase with benzylpenicillin. *J. Am. Chem. Soc. 127*, 4454−4465.
(198) Hermann, J. C., Ridder, L., Hotje, H. D., and Mulholland, A. J. (2006) Molecular mechanisms of antibiotic resistance: QM/MM modelling of deacylation in a class A beta-lactamase. *Org. Biomol. Chem. 4*, 206−210.
(199) Meroueh, S. O., Fisher, J. F., Schlegel, H. B., and Mobashery, S. (2005) Ab initio QM/MM study of class A beta-lactamase acylation:

Dual participation of Glu166 and Lys73 in a concerted base promotion of Ser70. *J. Am. Chem. Soc. 127*, 15397−15407.
(200) Hermann, J. C., Pradon, J., Harvey, J. N., and Mulholland, A. J. (2009) High Level QM/MM Modeling of the Formation of the Tetrahedral Intermediate in the Acylation of Wild Type and K73A Mutant TEM-1 Class A beta-Lactamase. *J. Phys. Chem. A 113*, 11984−11994.
(201) Tomanicek, S. J., Wang, K. K., Weiss, K. L., Blakeley, M. P., Cooper, J., Chen, Y., and Coates, L. (2011) The active site protonation states of perdeuterated Toho-1 [beta]-lactamase determined by neutron diffraction support a role for Glu166 as the general base in acylatio. *FEBS Lett. 585*, 364−368.
(202) Gherman, B. F., Goldberg, S. D., Cornish, V. W., and Friesner, R. A. (2004) Mixed quantum mechanical/molecular mechanical (QM/MM) study of the deacylation reaction in a penicillin binding protein (PBP) versus in a class C beta-lactamase. *J. Am. Chem. Soc. 126*, 7652−7664.
(203) My, N. H., Hirao, H., Van, D. U., and Morokuma, K. (2011) Computational Studies of Bacterial Resistance to beta-Lactam Antibiotics: Mechanism of Covalent Inhibition of the Penicillin-Binding Protein 2a (PBP2a). *J. Chem. Inf. Model. 51*, 3226−3234.
(204) Tripathi, R., and Nair, N. N. (2012) Thermodynamic and Kinetic Stabilities of Active Site Protonation States of Class C beta-Lactamase. *J. Phys. Chem. B 116*, 4741−4753.
(205) Fonseca, F., Chudyk, E. I., van der Kamp, M. W., Correia, A., Mulholland, A. J., and Spencer, J. (2012) The Basis for Carbapenem Hydrolysis by Class A β-Lactamases: A Combined Investigation using Crystallography and Simulations. *J. Am. Chem. Soc. 134*, 18275−18285.
(206) Oelschlaeger, P., Ai, N., DuPrez, K. T., Welsh, W. J., and Toney, J. H. (2010) Evolving Carbapenemases: Can Medicinal Chemists Advance One Step Ahead of the Coming Storm? *J. Med. Chem. 53*, 3013−3027.
(207) Dal Peraro, M., Llarrull, L. I., Röthlisberger, U., Vila, A. J., and Carloni, P. (2004) Water-assisted reaction mechanism of monozinc beta-lactamases. *J. Am. Chem. Soc. 126*, 12661−12668.
(208) Dal Peraro, M., Vila, A. J., Carloni, P., and Klein, M. L. (2007) Role of zinc content on the catalytic efficiency of B1 metallo beta-lactamases. *J. Am. Chem. Soc. 129*, 2808−2816.
(209) Spencer, J., Read, J., Sessions, R. B., Howell, S., Blackburn, G. M., and Gamblin, S. J. (2005) Antibiotic recognition by binuclear metallo-beta-lactamases revealed by X-ray crystallography. *J. Am. Chem. Soc. 127*, 14439−14444.
(210) Xu, D., Guo, H., and Cui, Q. (2007) Antibiotic Binding to Dizinc β-Lactamase L1 from *Stenotrophomonas maltophilia*: SCC-DFTB/CHARMM and DFT Studies. *J. Phys. Chem. A 111*, 5630−5636.
(211) Xu, D., Guo, H., and Cui, Q. (2007) Antibiotic deactivation by a dizinc beta-lactamase: Mechanistic insights from QM/MM and DFT studies. *J. Am. Chem. Soc. 129*, 10814−10822.
(212) Xu, D. G., Zhou, Y. Z., Xie, D. Q., and Guo, H. (2005) Antibiotic binding to monozinc CphA beta-lactamase from Aeromonas hydropila: Quantum mechanical/molecular mechanical and density functional theory studies. *J. Med. Chem. 48*, 6679−6689.
(213) Xu, D. G., Xie, D. Q., and Guo, H. (2006) Catalytic mechanism of class B2 metallo-beta-lactamase. *J. Biol. Chem. 281*, 8740−8747.
(214) Wu, S., Xu, D., and Guo, H. (2010) QM/MM Studies of Monozinc β-Lactamase CphA Suggest That the Crystal Structure of an Enzyme−Intermediate Complex Represents a Minor Pathway. *J. Am. Chem. Soc. 132*, 17986−17988.
(215) Garau, G., Bebrone, C., Anne, C., Galleni, M., Frère, J.-M., and Dideberg, O. (2005) A Metallo-[β]-lactamase Enzyme in Action: Crystal Structures of the Monozinc Carbapenemase CphA and its Complex with Biapenem. *J. Mol. Biol. 345*, 785−795.
(216) Gatti, D. L. (2012) Biapenem Inactivation by B2Metallo beta-Lactamases: Energy Landscape of the Post-Hydrolysis Reactions. *PLoS ONE 7*, No. e30079.
(217) Frushicheva, M. P., Warshel, A., and Cao, J. (2011) Challenges and advances in validating enzyme design proposals: The case of Kemp eliminase catalysis. *Biochemistry 50*, 3849−3858.
(218) Martí, S., Andrés, J., Silla, E., Moliner, V., Tuñón, I., and Bertrán, J. (2007) Computer-aided rational design of catalytic antibodies: The 1F7 case. *Angew. Chem., Int. Ed. 46*, 286−290.
(219) Martí, S., Andrés, J., Moliner, V., Silla, E., Tuñón, I., and Bertrán, J. (2008) Predicting an improvement of secondary catalytic activity of promiscuous isochorismate pyruvate lyase by computational design. *J. Am. Chem. Soc. 130*, 2894−2895.
(220) Lassila, J. K., Keeffe, J. R., Kast, P., and Mayo, S. L. (2007) Exhaustive mutagenesis of six secondary active-site residues in Escherichia coli chorismate mutase shows the importance of hydrophobic side chains and a helix N-capping position for stability and catalysis. *Biochemistry 46*, 6883−6891.
(221) Martí, S., Andrés, J., Moliner, V., Silla, E., Tuñón, I., and Bertrán, J. (2009) Mechanism and Plasticity of Isochorismate Pyruvate Lyase: A Computational Study. *J. Am. Chem. Soc. 131*, 16156−16161.
(222) Zheng, F., Yang, W. C., Ko, M. C., Liu, J. J., Cho, H., Gao, D. Q., Tong, M., Tai, H. H., Woods, J. H., and Zhan, C. G. (2008) Most efficient cocaine hydrolase designed by virtual screening of transition states. *J. Am. Chem. Soc. 130*, 12148−12155.
(223) Zheng, F., Yang, W. C., Xue, L., Hou, S. R., Liu, J. J., and Zhan, C. G. (2010) Design of High-Activity Mutants of Human Butyrylcholinesterase against (-)-Cocaine: Structural and Energetic Factors Affecting the Catalytic Efficiency. *Biochemistry 49*, 9113−9119.
(224) Xue, L., Ko, M. C., Tong, M., Yang, W. C., Hou, S. R., Fang, L., Liu, J. J., Zheng, F., Woods, J. H., Tai, H. H., and Zhan, C. G. (2011) Design, Preparation, and Characterization of High-Activity Mutants of Human Butyrylcholinesterase Specific for Detoxification of Cocaine. *Mol. Pharmacol. 79*, 290−297.
(225) Liu, J. J., and Zhan, C. G. (2012) Reaction Pathway and Free Energy Profile for Cocaine Hydrolase-Catalyzed Hydrolysis of (-)-Cocaine. *J. Chem. Theory Comput. 8*, 1426−1435.
(226) Zhan, C. G., and Gao, D. Q. (2005) Catalytic mechanism and energy barriers for butyrylcholinesterase-catalyzed hydrolysis of cocaine. *Biophys. J. 89*, 3863−3872.
(227) Pan, Y. M., Gao, D. Q., Yang, W. C., Cho, H., Yang, G. F., Tai, H. H., and Zhan, C. G. (2005) Computational redesign of human butyrylcholinesterase for anticocaine medication. *Proc. Natl. Acad. Sci. U. S. A. 102*, 16656−16661.
(228) Sun, H., Pang, Y.-P., Lockridge, O., and Brimijoin, S. (2002) Re-engineering Butyrylcholinesterase as a Cocaine Hydrolase. *Mol. Pharmacol. 62*, 220−224.
(229) Röthlisberger, D., Khersonsky, O., Wollacott, A. M., Jiang, L., DeChancie, J., Betker, J., Gallaher, J. L., Althoff, E. A., Zanghellini, A., Dym, O., Albeck, S., Houk, K. N., Tawfik, D. S., and Baker, D. (2008) Kemp elimination catalysts by computational enzyme design. *Nature 453*, 190−U194.
(230) Alexandrova, A. N., Röthlisberger, D., Baker, D., and Jorgensen, W. L. (2008) Catalytic mechanism and performance of computationally designed enzymes for Kemp elimination. *J. Am. Chem. Soc. 130*, 15907−15915.
(231) Debler, E. W., Ito, S., Seebeck, F. P., Heine, A., Hilvert, D., and Wilson, I. A. (2005) Structural origins of efficient proton abstraction from carbon by a catalytic antibody. *Proc. Natl. Acad. Sci. U. S. A. 102*, 4984−4989.
(232) Alexandrova, A. N., and Jorgensen, W. L. (2009) Origin of the activity drop with the E50D variant of catalytic antibody 34E4 for Kemp elimination. *J. Phys. Chem. B 113*, 497−504.
(233) Kiss, G., Röthlisberger, D., Baker, D., and Houk, K. N. (2010) Evaluation and ranking of enzyme designs. *Protein Sci. 19*, 1760−1773.
(234) Kumarasiri, M., Baker, G. A., Soudackov, A. V., and Hammes-Schiffer, S. (2009) Computational Approach for Ranking Mutant Enzymes According to Catalytic Reaction Rates. *J. Phys. Chem. B 113*, 3579−3583.
(235) Frushicheva, M. P., Cao, J., Chu, Z. T., and Warshel, A. (2010) Exploring challenges in rational enzyme design by simulating the

catalysis in artificial Kemp eliminase. *Proc. Natl. Acad. Sci. U. S. A. 107*, 16869−16874.
(236) Privett, H. K., Kiss, G., Lee, T. M., Blomberg, R., Chica, R. A., Thomas, L. M., Hilvert, D., Houk, K. N., and Mayo, S. L. (2012) Iterative approach to computational enzyme design. *Proc. Natl. Acad. Sci. U. S. A. 109*, 3790−3795.
(237) Burger, S. K., Thompson, D. C., and Ayers, P. W. (2011) Quantum mechanics/molecular mechanics strategies for docking pose refinement: distinguishing between binders and decoys in cytochrome c peroxidase. *J. Chem. Inf. Model. 51*, 93−101.
(238) Hsiao, Y. W., Drakenberg, T., and Ryde, U. (2005) NMR structure determination of proteins supplemented by quantum chemical calculations: Detailed structure of the Ca^{2+} sites in the EGF34 fragment of protein S. *J. Biomol. NMR 31*, 97−114.
(239) Yu, N., Hayik, S. A., Wang, B., Liao, N., Reynolds, C. H., and Merz, K. M. (2006) Assigning the protonation states of the key aspartates in beta-secretase using QM/MM X-ray structure refinement. *J. Chem. Theory Comput. 2*, 1057−1069.
(240) Li, X., Hayik, S. A., and Merz, K. M., Jr (2010) QM/MM X-ray refinement of zinc metalloenzymes. *J. Inorg. Biochem. 104*, 512−522.
(241) Pang, J. Y., Scrutton, N. S., de Visser, S. P., and Sutcliffe, M. J. (2010) Assignment of the Vibrational Spectra of Enzyme-Bound Tryptophan Tryptophyl Quinones Using a Combined QM/MM Approach. *J. Phys. Chem. A 114*, 1212−1217.
(242) Chung, J. Y., Chung, H. W., Cho, S. J., Hah, J. M., and Cho, A. E. (2010) QM/MM based 3D QSAR models for potent B-Raf inhibitors. *J. Comput.-Aided Mol. Des. 24*, 385−397.